

A COMPRESSIBLE FORMULATION FOR MULTIPHASE FLOWS OF GEOPHYSICAL AND GEODYNAMIC INTEREST

By

Lucas Gamertsfelder

A THESIS SUBMITTED TO MACQUARIE UNIVERSITY

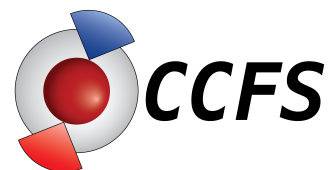
FOR THE DEGREE OF MASTER OF RESEARCH

DEPARTMENT OF EARTH AND PLANETARY SCIENCES

AUSTRALIAN RESEARCH COUNCIL CENTRE OF EXCELLENCE FOR

CORE TO CRUST FLUID SYSTEMS (CCFS) AND GEMOC

NOVEMBER 2017



EXAMINER'S COPY

© Lucas Gamertsfelder, 2017.

Typeset in L^AT_EX 2_ε.

Abstract

Multi-Phase Transport controls a number of important processes in the Earth's interior. Unfortunately, most available modelling platforms (and their underlying system of equations) are not well-suited to deal with the MPT nature of geological processes . The aim of this project is to develop a compressible Multi-Phase formulation able to handle the required level of complexity of both turbulent and non-turbulent natural systems. This platform will provide a unique and holistic understanding of key geological processes such as melt generation and migration, core formation, metasomatism, magma-chamber formation, ore generation and emplacement, and secular evolution of planetary bodies.

Declaration

I certify that the work in this thesis entitled “**A Compressible Formulation For Multiphase Flows of Geophysical and Geodynamic Interest**” has not previously been submitted for a degree, nor has it been submitted as partial requirement for a degree to any other university or institution other than Macquarie University.

I also verify that this thesis is an original piece of research and has been written by me. Any help and assistance that I have received in my research work and the preparation of the thesis itself have been properly acknowledged.

In addition, I certify that all data, information sources and literature used are indicated in the thesis.

Lucas Gamertsfelder

Student ID: 45097046

November 29, 2017

Contents

Abstract	v
Declaration	vii
List of Figures	xi
1 Introduction	1
2 Averaging Techniques	5
2.1 Purposes of Averaging	5
2.2 Ensemble Averaging	7
2.2.1 Defining the Ensemble Average	8
2.2.2 Averaging Application and Identities	11
3 Equations of Flow	13
3.1 Governing Equations	14
3.1.1 Mass Equation	14
3.1.2 Chemical Transport	16
3.1.3 Momentum Equation	16
3.1.4 Energy Equation	18
3.2 Viscous Stress Tensor	23
3.2.1 Newtonian Definition	23
3.2.2 Averaged Viscous Stress Tensor	25

3.3	Turbulence Modelling	28
3.3.1	Turbulent Stress	28
3.3.2	Turbulent Scalar Flux	29
3.3.3	Turbulent Energy Dissipation	29
3.3.4	Comparison of Turbulence Models	32
3.4	Interfacial Interactions	34
3.4.1	Interfacial Momentum Transport	34
3.4.2	Interfacial Energy Transport	37
3.5	Additional Laws	37
3.5.1	Murnaghan's Equation of State	37
3.5.2	Averaged Heat Flux	38
3.5.3	Pressure Difference	40
3.6	Summary	40
4	Examples	41
4.1	Model description	42
4.2	Results	43
4.2.1	Non-turbulent and incompressible formulation	43
4.2.2	Turbulent and incompressible formulation	44
4.2.3	Compressible formulation	44
5	Conclusion & Discussion	49
A	Averaging Properties	51
A.1	Interchanging Phase- and Mass-Weightings	51
A.2	Fluctuation Products	52
	References	55

List of Figures

2.1	Illustrative example of averaging techniques.	6
2.2	Illustration of Borel set definitions.	9
3.1	Illustration of the Reynolds decomposition of a turbulent field variable . . .	18
3.2	Illustration of a flat-plate boundary layer problem.	33
4.1	Evolution of $\#Mg$, temperature and phase abundance with no turbulence. .	46
4.2	Evolution of densities, velocities and pressures with no turbulence.	46
4.3	Evolution of velocities with turbulence.	47
4.4	Evolution of pressure differences with turbulence.	47
4.5	Evolution of temperature and phase abundance with compressibility.	48
4.6	Evolution of densities, velocities and pressures with compressibility.	48

1

Introduction

The interaction of multiple phases in natural flows, as well as how these interactions affect the bulk behaviour of the flows, are topics of great practical importance (e.g. modelling of nuclear reactors, extraction of oil and gas, modelling of pyroclastic flows, etc). Within the realm of the geosciences, multiphase flows are ubiquitous. For instance, when magma is generated at depth, it tends to move upwards due to its low relative density, percolating through a matrix of more or less viscous materials. The melt-matrix system can therefore be considered as a two-phase viscous system. The motion of magma in shallow levels of the crust is also a multiphase flow made up of gas bubbles, solid crystals and liquid. The eruption and collapse of pyroclastic are another two examples of a fluid composed of multiple interacting phases. These are just a few examples of relevance to geodynamics, geochemistry and geophysics.

The modelling of such flows requires a multiphase formulation of the governing equations. In the multiphase approach, there will generally be a discontinuity in field variables (velocity, density, etcetera) across the phases' boundaries. A way of dealing with this is by introducing boundary conditions between each phase, though it may be tedious, depending on the system's configuration, and must be repeated for each unique experiment. Additionally, turbulence effects may cause excitation in arbitrary directions. A useful technique which can alleviate both of these problems is *averaging*; it allows some generalizations to be made about interface transport, simplifying considerably the final formulation of the problem. Averaging techniques will be discussed in Chapter 2.

Multiphase and multicomponent flow in geodynamics is a relatively underdeveloped field. While today there are numerous textbooks describing the modelling of viscous, creeping flows in the geodynamic community (e.g. for mantle convection simulations), the same is not true for multiphase and/or multicomponent flows. Due to the inherent complexity of modelling multiple phases and the lack of experimental results to constrain formulations, multiphase flow models for n -phase, m -component systems have progressed relatively slowly. An important result from the geophysical community for two-phase incompressible flow came from McKenzie [1] who presented a Darcy energetic flow system applied to a partial melting example. Beginning from laws of conservation, the paper resulted in a one-dimensional compaction model from which practical numerical results were procured in the form of depth dependent plots.

This model was subsequently extended for multiple component flows [2][3] by introduction of a transport equation for concentration. This allowed chemical development, such as phase change information and evolution of system concentrations, to be studied. A change in independent variable is demonstrated possible by Spiegelman [4], who reforms McKenzie's equations to be pressure dependent.

Some years later, Bercovici, Ricard and Schubert presented a (volume) averaged two-phase model [5][6][7]. Their result had notable advantages over McKenzie's, among them: an more fundamental treatment of phase-phase momentum transport and flux, which does

not conform to Darcy’s law. However, this work was still restricted to two phases. Modifications were made later by Bercovici [8] and Sramek [9] which focused on improving the model for interfacial transfer terms. Particularly, the former paper studied the interface energy partitioning, while the second developed expressions for pressure drop interfacial mass transfer using phenomenological logic (see de Groot’s textbook [10]).

Recently, an n -phase m -component model was put forward by Oliveira et al. [11] based on the approach of ensemble averaging. In this model, each phase is explicitly modelled with its own balance equations, which are interrelated via interaction terms such as mass transfer due to phase change. Steps towards a sturdy numerical framework are taken, aimed at application in the Earth sciences.

In the literature cited so far, incompressibility is ultimately assumed and turbulence is neglected under the assumption of a Stokes’ flow, where all quantities are transported instantaneously.

The assumption of constant density is an inaccuracy of varying degrees in all cases. Particularly, it is significant in the case of liquid melt migration [12]. The use of turbulent-free equations is common in geodynamics due to small Reynolds number characterising many flows of interest. However, this assumption leaves out a large number of processes of geochemical, geophysical and geodynamic interest (e.g. the dynamics of magma chambers, volcanic eruptions, magma degassing and emplacement, rapid migration of large volumes of magma at shallow depths, among others). In these cases, it is of interest to implement turbulence models and find whether their neglect is justifiable.

This document presents an ensemble averaged compressible multi-phase multi-component system of equations including turbulence. In the second chapter, the volume, time and the ensemble averaging approaches will be introduced and described. In the third chapter, averaging techniques will be applied to a compressible n -phase, m -component system of equations, which are then completed using a set of averaged complementary models for stress, turbulence, interface transfer, and Fourier’s heat law and Murnaghan’s Equation of State. Finally, in the fourth chapter, the product of previous parts will be applied in some

examples to observe effects of compressibility and turbulence for comparison to results of McKenzie [1], Bercovici et al. [5] and Oliveira et al. [11].

2

Averaging Techniques

2.1 Purposes of Averaging

In three dimensional single-phase flow, boundary conditions are only specified on surfaces - the set of variables describing the system are continuous throughout the domain. When additional phases are introduced, however, each variable field has a discontinuity as it crosses the interface between phases due to the different physical properties in each phase. For example, the density field changes abruptly between a pond and the stone falling through it. Of two methods for dealing with these discontinuities, the first is to include jump conditions for each system parameter at the interface [13, p 31]. This may be useful for separated flows, but is very difficult to apply for the case of porous or dispersed media due to vast number of interfaces (however methods for capturing the interfaces have been studied [14]). Additionally, these conditions are only applicable in the experiment for which they were

formed. The second method is to replace the deterministic multi-boundary representation with a simpler representation and then use generic interface interaction models.

Turbulent motion is a second important reason to utilise an averaged system. In a turbulent flow, descriptive physical variables are excited arbitrarily in an infinite number of directions [15]. Hence, the fields are generally functions of an extremely complicated nature (i.e. there are many non-negligible Fourier expansion terms); it is practically impossible to describe the time-dependence of physical variables (Figure 3.1). In these cases, a statistical description is required, and an averaged system proves useful. An important consequence of averaging a k -phase system is that the k -phases then coexist with different probabilities, represented by a quantity ϕ_k , the phase density.

The three main averaging approaches for continuous phase equations are: time, volume and ensemble averaging (see Figure 2.1 for an illustrative example). A large number of studies have been conducted into each of these approaches, with Bercovici et al. [5][6][7] being one of the leading references for volume averaging in geodynamics; Ishii [16] investigating time-averaging extensively in his textbook and studies utilising ensemble averaging being largely

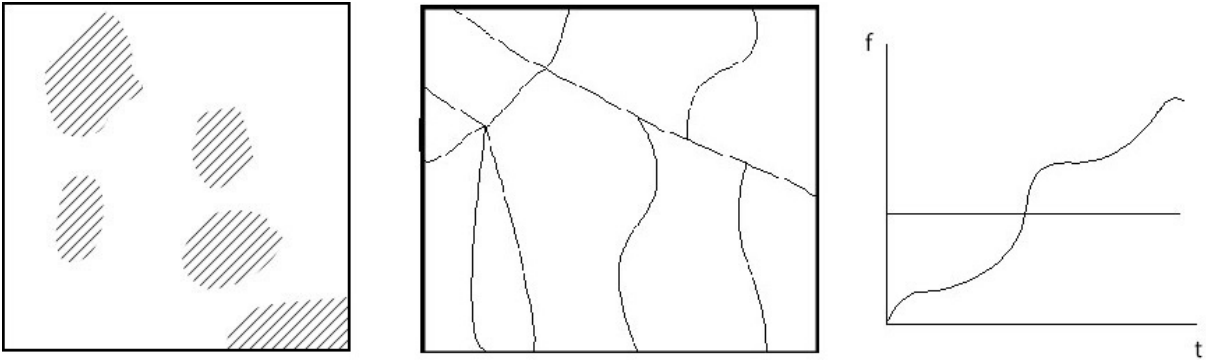


FIGURE 2.1: Illustrative representation of time, volume and ensemble averaging techniques. The first panel represents volume averaging. The blobs are solid grains embedded in a flowing fluid. This method of averaging integrates field properties over the volume of one phase and treats them as the averaged field variables. For instance, porosity is undefined at a point, but volume averaging can lend the point a value based on the neighbourhood it resides in. The second panel shows microscopic pore lines embedded in a solid is useful for viewing ensemble averaging. A fluid flowing through this system may take a variety of paths. Ensemble averaging takes the average flow and defines field variables based on that. The third panel is for time averaging and shows the value of a field variable measured over a certain interval of time. Time averaging will assign the value of the average of this field variable in the time interval as the averaged field variable (solid line).

developed by Drew and Passman [13][17] with applications taken into bubbly two-phase flows by Park, et al. [18], incompressible fluid-particle suspensions by Joseph et al. [19] and general multi-phase, multi-component reactive transports by Oliveira, et al. [11].

The ensemble average is taken over every imaginable structure and development of a system with set initial and boundary conditions. Hence, the time and volume averages are samples on the ensemble average [20]; representative in a statistical sense. The generality of it is attractive in the context of the numerous types of geophysical and geodynamic flows that can be tackled. Ensemble averaging is also less developed in geodynamics than its volume and time counterparts.

2.2 Ensemble Averaging

Given set boundary conditions, a range of flow configurations may be realised. This may be because of unobserved damage or alterations in the system, or simply due to the random nature of turbulence. "Ensemble averaging" is an average over the ensemble of these possible realizations of the flow. Consider the middle tile of Figure 2.1. The flow may travel through the volume using a number of paths; the exact one taken in separate, identical experiments is impossible to predict with total certainty. If there is some continuity in the flow (e.g. velocity) with the position and subsequent locations, then it may be reasonable to average over the paths for the flow properties when predicting the development of the system. That is, if taking a different path has a minor effect on the flow, then averaging over the *possible* paths will give an average flow in roughly the same direction as the exact flow. All realizations in the ensemble are equivalent in the averaged sense. This attribute lends repeatability to the flow system; at each repetition of the experiment, the probability of getting an exact repetition of a flow is practically zero, while we will always get another element in the average class.

2.2.1 Defining the Ensemble Average

The formalism of ensemble averaging will be presented following the method of Drew and Passman[13] and Drew[17], while using the textbook by Doob[21] as a reference.

Before presenting the definition of ensemble average, it is necessary to introduce a few definitions from measure theory. First

DEFINITION 1. *A collection of subsets \mathcal{S} is named an algebra if all of the following four properties hold,*

$$(1) \text{ the empty set belongs to } \mathcal{S}: \emptyset \in \mathcal{S} \quad (2.1)$$

$$(2) \mathcal{S} \text{ is closed under the complement: if } A \in \mathcal{S} \text{ then } A^c \in \mathcal{S} \quad (2.2)$$

$$(3) \mathcal{S} \text{ is closed under finite intersections: if } A_i \in \mathcal{S} \forall i = 1, 2, 3 \dots N \text{ then } \bigcap_i^N A_i \in \mathcal{S} \quad (2.3)$$

$$(4) \mathcal{S} \text{ is closed under finite unions: if } A_i \in \mathcal{S} \forall i = 1, 2, 3 \dots N \text{ then } \bigcup_i^N A_i \in \mathcal{S}. \quad (2.4)$$

and second,

DEFINITION 2. *An algebra \mathcal{S} of subsets of a space S is a σ -algebra if \mathcal{S} contains the limit of every monotone sequence of its sets. That is, for non-increasing $A_i \in \mathcal{S}$,*

$$\bigcap_{i \geq n} A_i \in \mathcal{S}$$

and non-decreasing $B_i \in \mathcal{S}$

$$\bigcup_{i \geq n} B_i \in \mathcal{S}$$

equivalently, one replaces property (3) and (4) of the algebra with closure under countable unions and intersections. Combined, (S, \mathcal{S}) is then called a measurable space, and the sets in \mathcal{S} called measurable.

then the class of Borel subsets may be defined.

DEFINITION 3. *The class of Borel subsets of a metric space S is the σ -algebra $\sigma(\mathbb{G}) = \sigma(\mathbb{F})$ where \mathbb{G} and \mathbb{F} are the classes of open and closed subsets of S^1 .*

¹by an inductive argument it is possible to construct the Borel subsets to be the smallest σ -algebra

Probabilities may be assigned naturally to Borel sets. Hence, these sets will be used to tie probabilities to realizations to prepare for averaging. The following subsets of the ensemble \mathcal{E} of realizations are defined as the collection of Borel sets

$$\bar{\mathcal{E}}(\mathbf{x}, t; F) = \{\mu | f(\mathbf{x}, t; \mu) \leq F\} \quad (2.5)$$

for all values of F , where f is a parameter of the system, e.g. velocity or density, μ is a realization and $\bar{\mathcal{E}}$ is the ensemble. This definition says that the set $\bar{\mathcal{E}}$ is the collection of realizations μ such that, for instance, the velocity $\mathbf{v} \leq F$. As F increases, the number of realizations in $\bar{\mathcal{E}}$ monotonically increases. These can be used to construct the desired minimal Borel sets

$$d\bar{\mathcal{E}}(\mathbf{x}, t; F, F + dF) = \bar{\mathcal{E}}(\mathbf{x}, t, F + dF) \cap \bar{\mathcal{E}}(\mathbf{x}, t, F) \quad (2.6)$$

This set is the slice of realizations of the variable f within $(F, F + dF)$ (See Figure (2.2)). The union of all of these slices must equal $\bar{\mathcal{E}}$. Another useful set is defined

$$d\underline{\mathcal{E}}(f^*, dF) = \left\{ \mu \left| \max_{(\mathbf{x}, \mathbf{t})} |f(\mathbf{x}, t; \mu) - f^*(\mathbf{x}, \mathbf{t})| \leq dF \right. \right\}. \quad (2.7)$$

containing the open sets. If it is not already, then remove the intersection of all of the subsets in the class. Assume there is a smaller class of Borel subsets, and then show that it does not contain an element in the original set S . Thus, we can assume that our Borel subsets are the made up of the smallest open sets.

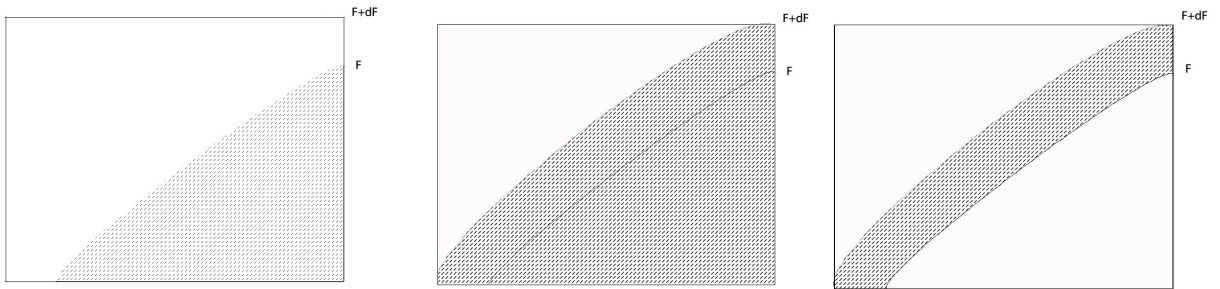


FIGURE 2.2: The above figure illustrates the intersection of the two sets $\bar{\mathcal{E}}^c(\mathbf{x}, t, F)$ and $\bar{\mathcal{E}}(\mathbf{x}, t, F + dF)$. The shaded space represents the fraction of realizations in the ensemble which the sets encompass, where the entire box represents the ensemble. The first tile represents $\bar{\mathcal{E}}(\mathbf{x}, t, F)$, the second $\bar{\mathcal{E}}(\mathbf{x}, t, F + dF)$, and the third $\bar{\mathcal{E}}(\mathbf{x}, t, F + dF) \cap \bar{\mathcal{E}}(\mathbf{x}, t, F)$. Note that if one takes dF small enough, the intersection will be an infinitely small slice, yet the union of them will represent the ensemble.

The above equation represents the set of realizations such that the function $f(\mathbf{x}, t; \mu)$ is within dF of the function $f^*(\mathbf{x}, \mathbf{t})$. Keep in mind that these functions may be density ρ , velocity, \mathbf{v} or any other field quantity. As we are finding the average of parameter f , we need to define the probability measure m on \mathcal{E} . It is a finite measure

DEFINITION 4. *A finite measure λ is a mapping on an algebra \mathcal{S} to a subset of the extended real line $\overline{\mathbb{R}} = \mathbb{R} \cup -\infty, +\infty$, either $[-\infty, \infty)$ or $(-\infty, \infty]$ that is countably additive. That is,*

$$\lambda\left(\bigcup A_i\right) = \sum_i \lambda(A_i) \quad (2.8)$$

where A_i are a disjoint, infinite sequence of sets belonging to \mathcal{S} .

with the additional properties,

- (1) $m(S) = 1$;
- (2) m is monotone, i.e. : if $\overline{\mathcal{E}}_1, \overline{\mathcal{E}}_2 \in \overline{\mathcal{E}}$ and $\overline{\mathcal{E}}_1 \subset \overline{\mathcal{E}}_2$ then $m(\overline{\mathcal{E}}_1) \leq m(\overline{\mathcal{E}}_2)$
- (3) m is countably additive, i.e. : for any sequence of disjoint sets $\overline{\mathcal{E}}_1, \overline{\mathcal{E}}_2, \dots, \overline{\mathcal{E}}_n, \dots$ one has

$$\mu\left(\bigcup_{n=1}^{\infty} \overline{\mathcal{E}}_n\right) = \sum_{n=1}^{\infty} \mu(A_n).$$

the probability $m(S)$ is then defined on the sets $\overline{\mathcal{E}}$ and $d\overline{\mathcal{E}}$. For instance, $m(\overline{\mathcal{E}})$ with $f = \rho$ is the probability that the density, $\rho \leq F$ (that is, the element $\mu_1 \in \overline{\mathcal{E}}$ is realised). Similarly, $m(d\overline{\mathcal{E}})$ would represent the probability that ρ is in $(F, F + dF)$. Finally, the function $m(d\mathcal{E}(f^*, dF))$ is the probability that f is within dF of the arbitrary function f^* (using $\sup |f - dF|$ as a measure of distance).

Using the definition (2.7), the average of a function f can now be defined

$$\bar{f}(\mathbf{x}, t) = \lim_{N \rightarrow \infty} \sum_{i=1}^{N-1} F_i m(d\mathcal{E}(\mathbf{x}, t; F_i, dF_i)) \quad (2.9)$$

where

$$-\infty < F_1 < F_2 < \dots < F_N < \infty \quad (2.10)$$

and $dF_i = F_{i+1} - F_i$.

As $N \rightarrow \infty$, the ensemble is partitioned into slices at each value of F_i . The average of

f is defined as the sum of the multiple of probability of each outcome by that outcome's respective f value. \bar{f} in Equation 2.9 thus may be interpreted as the average value of f . The ensemble average may also be defined in terms of integral notation:

$$\langle f \rangle(\mathbf{x}, t) = \int_{\mathcal{E}} f(\mathbf{x}, t; \mu) dm(\mu). \quad (2.11)$$

This is essentially the same definition as (2.9) but using an integral instead with the density $dm(\mu) = d\bar{\mathcal{E}}(\mathbf{x}, t; F, F + dF)$: the probability that f is in $(F, F + dF)$.

2.2.2 Averaging Application and Identities

In Chapter 3, the postulated conservation equations will be reduced to phase-specific averaged models by first separating the equations by multiplying by a phase characteristic function and then ensemble averaging by using Equation (2.11).

To split the governing equations into a set of equations for each phase k , they will be multiplied by a characteristic function χ_k

$$\chi_k(\mathbf{x}, t; \mu) = \begin{cases} 1, & \text{if } \mathbf{x} \in k \text{ in realization } \mu \\ 0, & \text{if otherwise} \end{cases} \quad (2.12)$$

χ_k is a tool to pick out the k 'th phase from the total system by essentially equaling zero elsewhere. For instance, where ρ is density, $\chi_k \rho(x, y)$ is non-zero only in phase k , thus represents the k 'th phase density. In the next section its use will be demonstrated.

As averaged values are defined differently to non-averaged quantities, it is necessary to introduce a variety of equalities that hold for averaged variables. The following three are called the Reynolds' rules [17]:

$$\langle f + g \rangle = \langle f \rangle + \langle g \rangle \quad (2.13)$$

$$\langle \langle f \rangle g \rangle = \langle f \rangle \langle g \rangle \quad (2.14)$$

$$\langle c \rangle = c \quad (2.15)$$

for functions f and g and constants c , and the two below are named the Leibniz' rule and Gauss' rule [17] respectively, and they hold as long as the function is *well-defined*. This

condition is necessary since, by the definition of an average, differentiation and integration operations are being exchanged. For instance, in a closed 2D space $(x, y) \in [a, b] \times [c, d]$, $f(x, y)$ and $\frac{\partial f(x, y)}{\partial x}$ must be continuous in variables x and y ².

$$\left\langle \frac{\partial f}{\partial t} \right\rangle = \frac{\partial}{\partial t} \langle f \rangle \quad (2.16)$$

$$\left\langle \frac{\partial f}{\partial x_i} \right\rangle = \frac{\partial}{\partial x_i} \langle f \rangle \quad (2.17)$$

these results will be useful when manipulating the averaged equations of flow. They allow the averaging of derivatives without introducing an additional variable, e.g. $\langle \frac{\partial f}{\partial t} \rangle$. Finally there is the so-called topological equation

$$\rho \frac{\partial \chi_k}{\partial t} + \rho \mathbf{v}_i \cdot \nabla \chi_k = 0 \quad (2.18)$$

where \mathbf{v}_i is the interface velocity. Thus the above states that the material derivative of the characteristic function on the interface is always zero. When considering a point on the interior of a phase k , χ_k is either 0 or 1 implying the derivatives of χ_k are zero. Now at a point on the interface, there is a jump in χ_k . Since the material derivative tracks the trajectory of a point with time, and the jump in χ_k at that point on the interface remains the *same* as time progresses, the material derivative of a point on the interface must be zero. Hence the material derivative of χ_k is zero in all cases and the above equation holds.

²For those interested in the specifics, the definition of a well-defined function, check out the premise of the integral rule at this [hyperlink](#); otherwise, it simply indicates that the function has a few nice properties that allow it to be integrated over with little worry.

3

Equations of Flow

The averaging technique introduced in the previous chapter is applied in the following to present a closed system of balance equations governing fluid flow; particularly of mass, force and internal energy. The equations will describe compressible flow and be averaged over the set of possible realizations. Either of the sets of variables $(\langle \mathbf{v} \rangle_\rho, \langle p \rangle_\chi, \langle T \rangle_\rho)$ or $(\langle \mathbf{v} \rangle_\rho, \langle p \rangle_\chi, \langle s \rangle_\rho)$ where \mathbf{v} is velocity, p is thermodynamic pressure (see Section 3.2 for discussion of this pressure), T is temperature, s is specific entropy, may be used, depending on the how the energy equation is developed. The governing equations are to be first presented in an averaged form, then closed by presenting models for the unknown variables: the constitutive laws. The following notation is used throughout the text:

1. Ensemble Average of variable θ : $\langle \theta \rangle$

2. Phase-weighted Ensemble Average of variable θ

$$\langle \theta \rangle_\chi = \frac{\langle \chi_k \theta \rangle}{\langle \chi_k \rangle} \quad (3.1)$$

3. Mass-weighted Ensemble Average of variable θ :

$$\langle \theta \rangle_\rho = \frac{\langle \chi_k \rho \theta \rangle}{\langle \chi_k \rangle \langle \rho \rangle_\chi} \quad (3.2)$$

where θ is some field variable, ρ is density and χ_k is the phase characteristic function which is 1 in phase k and 0 otherwise. Note that the phase and mass-weighted averages are phase-specific because the characteristic function χ_k is implicit in them. Taking instead a mass or phase-weighted average of a governing variable in place of the usual average greatly helps in simplifying equations by reducing average of products into products of averages¹.

Additionally, on occasion it is suitable to use the notation

$$\langle f \rangle_\rho = \mathbf{f}_k \quad (3.3)$$

or

$$\langle g \rangle_\chi = \mathbf{g}_k \quad (3.4)$$

where f and g are some field variables. Note that the left hand side of both of the above equations are phase specific because of the χ_k present in the definitions 3.1 and 3.2. The right-hand side notation is useful when different phase variables must be compared.

3.1 Governing Equations

3.1.1 Mass Equation

The first and most simple of the governing equations is the conservation of mass. It is a postulate from physics which simply states that in a closed system, there can be no loss of total mass. However, it will be seen that for the phase-specific equations, there may be a loss of mass attributed to mass undergoing phase change (melting, boiling, etc.). The

¹for instance, density ρ is often in a product with velocity \mathbf{v} due to the definition of momentum. Thus, using the definitions, $\langle \rho \mathbf{v} \rangle$ becomes $\langle \rho \rangle \langle \mathbf{v} \rangle_\rho$ - a product of averages rather than average of products.

Eulerian reference frame is used, meaning that the balance equation considers fixed points, rather than moving particles (which is the domain of the *Lagrangian* reference frame).² The statement for total mass conservation is as follows

$$\frac{\partial \rho}{\partial t} + \nabla \cdot \rho \mathbf{v} = 0 \quad (3.5)$$

The first term describes local changes in the mass with time, while the second term represents advective changes. The above equation states that, at a particular point, the change in mass with time is negative the amount of mass leaving the point with velocity \mathbf{v} .

Breaking the total mass equation (3.5) down into k phase-specific equations by multiplication of a phase characteristic function (Equation (2.12)) and then ensemble averaging

$$\langle \chi_k \frac{\partial \rho}{\partial t} + \chi_k \nabla \cdot \rho \mathbf{v} \rangle = 0 \quad (3.6)$$

bringing χ_k into the derivatives by use of the product rule, and using linearity of ensemble average (i.e. linearity of integration)

$$\langle \frac{\partial \chi_k \rho}{\partial t} \rangle + \langle \nabla \cdot \chi_k \rho \mathbf{v} \rangle - \langle \rho \frac{\partial \chi_k}{\partial t} \rangle - \langle \rho \mathbf{v} \cdot \nabla \chi_k \rangle = 0. \quad (3.7)$$

Two observations from Drew and Passman [13] are now utilised for the above equation. The first is that ensemble averages and partial derivatives can be interchanged by use of the Leibniz rule (2.16). The second is the topological equation, Equation 2.18, which says

$$\rho \frac{\partial \chi_k}{\partial t} = -\rho \mathbf{v}_i \cdot \nabla \chi_k$$

$$\frac{\partial \langle \chi_k \rangle \langle \rho \rangle_\chi}{\partial t} + \langle \nabla \cdot \chi_k \rho \mathbf{v} \rangle + \langle \rho \mathbf{v}_i \cdot \nabla \chi_k \rangle - \langle \rho \mathbf{v} \cdot \nabla \chi_k \rangle = 0 \quad (3.8)$$

Hence, the averaged phase-specific mass equation is

$$\frac{\partial \langle \chi_k \rangle \langle \rho \rangle_\chi}{\partial t} + \nabla \cdot \langle \chi_k \rangle \langle \rho \rangle_\chi \langle \mathbf{v} \rangle_\rho = \Gamma_{m,k} \quad (3.9)$$

where $\Gamma_k = \langle \rho (\mathbf{v} - \mathbf{v}_i) \cdot \nabla \chi_k \rangle$. An additional term (on the right-hand side) has appeared due to the introduction of χ_k into the equation of mass (3.5). The term on the right-hand side is only non-zero on the interface (where $\nabla \chi_k \neq 0$). Thus, it is interpreted to represent mass transfer between phases.

²there's an interesting alignment between choice of reference frame and the method of solving homogeneous transport equations. To solve the equation $u_t + cu_x = 0$ for $u(x, t)$, one takes transformation of variables $\xi = x - ct$, reducing the equation to $v_t = 0$ where $v(\xi, t) = u(x, t)$. Notice that the new coordinates are moving coordinates, the analogy of the Lagrangian form.

3.1.2 Chemical Transport

The chemical balance equation behaves comparably to the mass because it describes a variable very similar: concentration. However, instead of having N equations for N phases, there will be $N \times M$, where M is the number of unique chemical components. This set of equations will give chemical evolution in the system, additionally providing information on the mass transfer rate Γ , as phase changes can occur as a consequence of chemical reactions. The non-averaged set of chemical transport equations is given by

$$\frac{\partial \rho c^b}{\partial t} + \nabla \cdot \rho c^b \mathbf{v} = 0 \quad (3.10)$$

where c^b is the concentration of component b . Splitting by phase and then averaging

$$\left\langle \chi_k \frac{\partial \rho c^b}{\partial t} + \chi_k \nabla \cdot \rho c^b \mathbf{v} \right\rangle = 0 \quad (3.11)$$

once again using the topological equation as well as linearity of the ensemble average

$$\frac{\partial \langle \chi_k \rangle \langle \rho \rangle_\chi \langle c^b \rangle}{\partial t} + \nabla \cdot \langle \chi_k \rangle \langle \rho \rangle_\chi \langle c^b \rangle_\rho \langle \mathbf{v} \rangle_\rho = \Gamma_{b,k} \quad (3.12)$$

where $\Gamma^b = \langle \rho c^b (\mathbf{v} - \mathbf{v}_i) \cdot \nabla \chi_k \rangle$ measures the amount of component c^b is changing phase due to chemical reaction. This value may be estimated through knowledge of the chemical reaction taking place.

3.1.3 Momentum Equation

The momentum conservation equation is a statement of Newton's Second Law: the physical postulate that the change in momentum is equal to the sum of forces on the system:

$$\frac{\partial \rho \mathbf{v}}{\partial t} + \nabla \cdot (\rho \mathbf{v} \mathbf{v}) = \nabla \cdot \boldsymbol{\sigma} + \rho \mathbf{b}. \quad (3.13)$$

On the left-hand side there is the sum of the local and advective changes in momentum. On the right-hand side, there are surface forces $\nabla \cdot \boldsymbol{\sigma}$ summed with body forces $\rho \mathbf{b}$. Multiplying by the characteristic function and ensemble averaging Equation (3.13)

$$\langle \chi_k \frac{\partial \rho \mathbf{v}}{\partial t} \rangle + \langle \chi_k \nabla \cdot (\rho \mathbf{v} \mathbf{v}) \rangle = \langle \chi_k \nabla \cdot \boldsymbol{\sigma} \rangle + \langle \chi_k \rho \mathbf{b} \rangle \quad (3.14)$$

taking the same steps as in the mass equation (3.6): moving χ_k inside the derivatives, using the topological equation as well as interchanging derivative and ensemble average operators

$$\frac{\partial \langle \chi_k \rangle \langle \rho \rangle_\chi \langle \mathbf{v} \rangle_\rho}{\partial t} + \nabla \cdot \langle \chi_k \rho \mathbf{v} \mathbf{v} \rangle = \nabla \cdot \langle \chi_k \sigma \rangle + \langle \chi_k \rangle \langle \rho \rangle_\chi \langle \mathbf{b} \rangle_\rho - \langle \rho \mathbf{v} [(\mathbf{v} - \mathbf{v}_i) - \sigma] \cdot \nabla \chi_k \rangle. \quad (3.15)$$

As opposed to mass conservation, the momentum equation has the non-linear term $\chi_k \rho \mathbf{v} \mathbf{v}$. This presents a problem because $\langle \chi_k \rho \mathbf{v} \mathbf{v} \rangle$ is in neither of the sets of the variables mentioned at the beginning of the chapter; to close the system this average of products will be reduced to a product of averages. A method for this comes from applying the Reynolds expansion: $\theta = \langle \theta \rangle + \theta''$ where θ is some field variable in some realization of the ensemble with that is the sum of the average $\langle \theta \rangle$ and fluctuation from the average θ'' (see Figure 3.1).

Expanding the velocities in the non-linear term

$$\begin{aligned} \frac{\partial \langle \chi_k \rangle \langle \rho \rangle_\chi \langle \mathbf{v} \rangle_\rho}{\partial t} + \nabla \cdot \langle \chi_k \rho (\langle \mathbf{v} \rangle_\rho + \mathbf{v}'') (\langle \mathbf{v} \rangle_\rho + \mathbf{v}'') \rangle &= \nabla \cdot \langle \chi_k \sigma \rangle + \langle \chi_k \rangle \langle \rho \rangle_\chi \langle \mathbf{b} \rangle_\rho \\ &\quad - \langle \rho \mathbf{v} [(\mathbf{v} - \mathbf{v}_i) - \sigma] \cdot \nabla \chi_k \rangle. \end{aligned} \quad (3.16)$$

The Reynolds expansion taken for velocity was mass-weighted $\mathbf{v} = \langle \mathbf{v} \rangle_\rho + \mathbf{v}''_\rho$ and the subscript on the fluctuation term will be omitted for convenience. The results of Appendix A.2 provide the method of dealing with the product of Reynolds expansions. The averaged, phase-weighted momentum equation becomes

$$\begin{aligned} \underbrace{\frac{\partial \langle \chi_k \rangle \langle \rho \rangle_\chi \langle \mathbf{v} \rangle_\rho}{\partial t}}_{(M1)} + \underbrace{\nabla \cdot \langle \chi_k \rangle \langle \rho \rangle_\chi \langle \mathbf{v} \rangle_\rho \langle \mathbf{v} \rangle_\rho}_{(M2)} &= \underbrace{\nabla \cdot \langle \chi_k \sigma \rangle}_{(M3)} - \underbrace{\nabla \cdot \langle \chi_k \rho \mathbf{v}'' \mathbf{v}'' \rangle}_{(M4)} \\ &\quad + \underbrace{\langle \chi_k \rangle \langle \rho \rangle_\chi \langle \mathbf{b} \rangle_\rho}_{(M5)} + \underbrace{\mathbf{M}_k}_{(M6)}. \end{aligned} \quad (3.17)$$

where all elements of this equation are detailed below

(M1) represents the local changes in average momentum.

(M2) is the advective changes in momentum

(M3) represents the averaged surface forces acting on the system. σ is the surface stress, whose model will be discussed in Section 3.2.

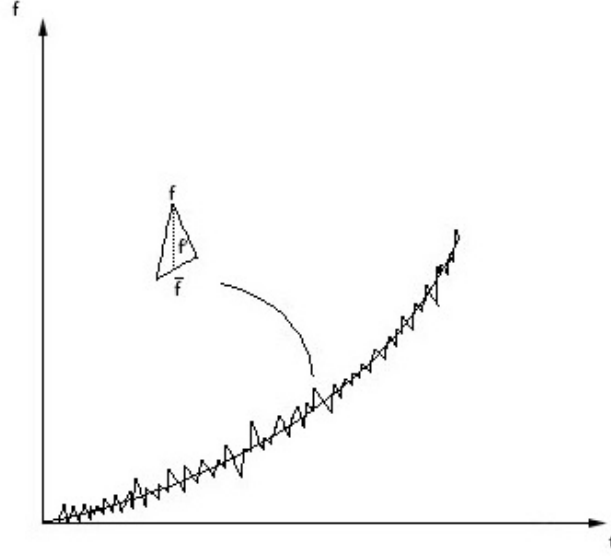


FIGURE 3.1: Where f is a field variable the above plot illustrates the definition of the Reynolds decomposition. f' (the dotted line) is defined as the difference between the actual variable f and averaged variable \bar{f} .

(M4) is the turbulent momentum flux, also commonly called Reynolds stress. Notice that it appears as a by-product of averaging. Terms like this are representative of chaotic motion in the system that may occur, and is one of the reasons averaging is useful; that the effects of *turbulence* may be isolated. Section 3.3 is dedicated to modelling turbulent terms.

(M5) represents the body forces on the system. In most cases, \mathbf{b} is replaced with gravity \mathbf{g} .

(M6) appears as a result of phase-splitting the total momentum equation and represents the transport of momentum across the interface. Section 3.4 is concerned with modelling interface terms.

3.1.4 Energy Equation

The classical conservation of internal energy equation is a balance between changes in specific internal energy with heat and work sources

$$\frac{\partial \rho u}{\partial t} + \nabla \cdot \rho \mathbf{v} u = -\nabla \cdot \mathbf{q} + Q + \sigma : \nabla \mathbf{v} \quad (3.18)$$

where u is internal energy, \mathbf{q} is surface heat flux, Q accounts for volume heat sources (e.g. radioactive decay) and $\sigma : \nabla \mathbf{v}$ represents the work done by surface stresses. The left-hand side may be re-expressed by use of the mass conservation equation (3.5) (employed in the first term on the right-hand side below)

$$\begin{aligned} \frac{\partial \rho u}{\partial t} + \nabla \cdot \rho \mathbf{v} u &= u \left(\frac{\partial \rho}{\partial t} + \nabla \cdot \rho \mathbf{v} \right) + \rho \frac{\partial u}{\partial t} + \rho \mathbf{v} \cdot \nabla u \\ &= \rho \left(\frac{\partial u}{\partial t} + \mathbf{v} \cdot \nabla u \right) \end{aligned} \quad (3.19)$$

this provides a form in which laws of thermodynamics may be readily incorporated. The thermodynamic pressure term may be extracted from the work on the right-hand side of (3.18) like so³

$$\rho \left(\frac{\partial u}{\partial t} + \mathbf{v} \cdot \nabla u \right) = -\nabla \cdot \mathbf{q} + Q - p \nabla \cdot \mathbf{v} + \boldsymbol{\tau} : \nabla \mathbf{v} \quad (3.20)$$

where $\boldsymbol{\tau} = \xi \text{tr}(\boldsymbol{\epsilon}) \mathbf{I} + 2\mu \boldsymbol{\epsilon}'$ is the stress tensor minus the thermodynamic pressure term $-p \mathbf{I}$ (see the Section 3.2). Instead of taking specific internal energy as a variable, specific entropy s or temperature T will be adopted. Assuming local thermodynamic equilibrium (means?) in the thermodynamic processes,⁴ internal energy may be expressed by using the first and second laws of thermodynamics (for instance, see Ricard's [22])

$$du = T ds - p d(\rho)^{-1} \quad (3.21)$$

$$du = c_v dT - (p + T \left(\frac{\partial p}{\partial T} \right)_v) d(\rho)^{-1} \quad (3.22)$$

where c_v is specific heat capacity at constant volume (i.e. amount of heat required for a change in temperature at constant volume). Substituting the entropy equation (3.21) into

³ That $-p \mathbf{I} : \nabla \mathbf{v} = -p \nabla \cdot \mathbf{v}$ can be easily verified:
$$\begin{pmatrix} p & 0 & 0 \\ 0 & p & 0 \\ 0 & 0 & p \end{pmatrix} : \begin{pmatrix} \frac{\partial v_1}{\partial x_1} & \frac{\partial v_1}{\partial x_2} & \frac{\partial v_1}{\partial x_3} \\ \frac{\partial v_2}{\partial x_1} & \frac{\partial v_2}{\partial x_2} & \frac{\partial v_2}{\partial x_3} \\ \frac{\partial v_3}{\partial x_1} & \frac{\partial v_3}{\partial x_2} & \frac{\partial v_3}{\partial x_3} \end{pmatrix} = p \frac{\partial v_1}{\partial x_1} + p \frac{\partial v_2}{\partial x_2} +$$

$p \frac{\partial v_3}{\partial x_3} = p \nabla \cdot \mathbf{v}.$

⁴which is rather bold for geodynamic processes, e.g. consider volcanic eruptions, low viscosity magma chambers, etc.

(3.20) and once again using the mass equation (and applying the chain rule)

$$\begin{aligned}\rho T \left(\frac{\partial s}{\partial t} + \mathbf{v} \cdot \nabla s \right) - \rho p \left(\frac{\partial(\rho)^{-1}}{\partial t} + \mathbf{v} \cdot \nabla(\rho)^{-1} \right) &= -\nabla \cdot \mathbf{q} + Q - p \nabla \cdot \mathbf{v} + \boldsymbol{\tau} : \nabla \mathbf{v} \\ \rho T \left(\frac{\partial s}{\partial t} + \mathbf{v} \cdot \nabla s \right) + \frac{p}{\rho} \left(\frac{\partial \rho}{\partial t} + \mathbf{v} \cdot \nabla \rho \right) &= -\nabla \cdot \mathbf{q} + Q - p \nabla \cdot \mathbf{v} + \boldsymbol{\tau} : \nabla \mathbf{v} \quad (3.23) \\ \rho T \left(\frac{\partial s}{\partial t} + \mathbf{v} \cdot \nabla s \right) + \frac{p}{\rho} (-\rho \nabla \cdot \mathbf{v}) &= -\nabla \cdot \mathbf{q} + Q - p \nabla \cdot \mathbf{v} + \boldsymbol{\tau} : \nabla \mathbf{v}\end{aligned}$$

and on cancelling the pressure terms on both sides

$$\rho T \left(\frac{\partial s}{\partial t} + \mathbf{v} \cdot \nabla s \right) = -\nabla \cdot \mathbf{q} + Q + \boldsymbol{\tau} : \nabla \mathbf{v} \quad (3.24)$$

reverting back to a form similar to Equation (3.18) using mass conservation

$$T \left(\frac{\partial \rho s}{\partial t} + \nabla \cdot \rho \mathbf{v} s \right) = -\nabla \cdot \mathbf{q} + Q + \boldsymbol{\tau} : \nabla \mathbf{v}. \quad (3.25)$$

An equation for temperature can be derived similarly using Equation (3.22)

$$c_v \left(\frac{\partial \rho T}{\partial t} + \nabla \cdot \rho \mathbf{v} T \right) = -\nabla \cdot \mathbf{q} + Q + \boldsymbol{\tau} : \nabla \mathbf{v} + \alpha K_T \nabla \cdot \mathbf{v}. \quad (3.26)$$

where K_T is the isothermal compressibility and α is the thermal expansiveness. The last term represents heat transfer due to isothermal processes, where instead of a change in temperature, expansion or compaction occurs. This term is zero for the incompressible case because compaction cannot occur.

The aim of this chapter is to present two closed systems of equations for modelling averaged multi-phase, multi-component flow using variables $(\langle \mathbf{v} \rangle_\rho, \langle p \rangle_\chi, \langle s \rangle_\rho)$ and $(\langle \mathbf{v} \rangle_\rho, \langle p \rangle_\chi, \langle T \rangle_\rho)$. With that in mind, averaged multi-phase versions of both Equations (3.25) and (3.26) are desirable. To avoid modelling complicated turbulence terms, an assumption is required for both the entropy and temperature equations. Particularly, consider a mass-weighted Reynolds Expansion of temperature

$$\begin{aligned}T &= \langle T \rangle_\rho + T''_\rho \\ \frac{T}{\langle T \rangle_\rho} &= 1 + \frac{T''_\rho}{\langle T \rangle_\rho}.\end{aligned}$$

If the fluctuation term T''_ρ is small with respect to $\langle T \rangle_\rho$, then T may be interchanged with $\langle T \rangle_\rho$. This is the assumption that will be taken for the entropy equation. An analogous

assumption $c_v'' = 0$ is taken for the temperature equation (3.26). With respect to each experiment under identical conditions, the temperature and specific heat capacity are assumed constant. The entropy equation (3.25) becomes

$$\left\langle \chi_k T \left(\frac{\partial \rho s}{\partial t} + \nabla \cdot \rho \mathbf{v} s \right) \right\rangle = -\langle \chi_k \nabla \cdot \mathbf{q} \rangle + \langle \chi_k Q \rangle + \langle \chi_k \boldsymbol{\tau} : \nabla \mathbf{v} \rangle \quad (3.27)$$

on bringing χ_k inside derivatives by use of the product rule and taking T out of the average (since $T \approx \langle T \rangle_\rho$)

$$T \left\langle \left(\frac{\partial \chi_k \rho s}{\partial t} + \nabla \cdot \chi_k \rho \mathbf{v} s - [\rho s (\mathbf{v} - \mathbf{v}_i) \cdot \nabla \chi_k] \right) \right\rangle = -\langle \nabla \cdot \chi_k \mathbf{q} \rangle + \langle \mathbf{q} \cdot \nabla \chi_k \rangle + \langle \chi_k Q \rangle + \langle \chi_k \boldsymbol{\tau} : \nabla \mathbf{v} \rangle \quad (3.28)$$

and taking the following steps

1. using the linearity property of the ensemble average
2. split the non-linear terms by use of Reynolds expansions
3. apply the definition of mass and phase-weighted averages (e.g. $\langle \rho \rangle_\chi = \frac{1}{\langle \chi_k \rangle} \langle \chi_k \rho \rangle$; see Equations 3.1 and 3.2)
4. group the interfacial terms on the right-hand side

results in the below equation

$$\underbrace{T \left(\frac{\partial \langle \chi_k \rangle \langle \rho \rangle_\chi \langle s \rangle_\rho}{\partial t} + \nabla \cdot \langle \chi_k \rangle \langle \rho \rangle_\chi \langle \mathbf{v} \rangle_\rho \langle s \rangle_\rho \right)}_{(S1)} = \underbrace{-\nabla \cdot \langle \chi_k \rangle \langle \mathbf{q} \rangle_\chi}_{(S2)} + \underbrace{\langle \chi_k \boldsymbol{\tau} \rangle : \nabla \langle \mathbf{v} \rangle_\rho}_{(S3)} \\ + \underbrace{\langle \chi_k \rangle \langle Q \rangle_\chi}_{(S4)} + \underbrace{\langle \chi_k \boldsymbol{\tau}'' : \nabla \mathbf{v}'' \rangle}_{(S5)} + \underbrace{\nabla \cdot \langle \chi_k \rho \mathbf{v}'' s'' \rangle}_{(S6)} \\ + \underbrace{\langle [\rho s (\mathbf{v} - \mathbf{v}_i) + \mathbf{q}] \cdot \nabla \chi_k \rangle}_{(S7)}. \quad (3.29)$$

where from left to right each term represents

(S1) represents the standard Eulerian transport of the averaged specific entropy.

(S2) is the averaged heat flux through the surface. This term can be modelled as proportional to a gradient in temperature by using Fourier's heat law (see Equation (3.86)).

(S3) is the work dissipation caused by viscous stress acting on the system. The derivation and discussion for the stress tensor is given in Section 3.2.

(S4) is the internal heating in the system which can be assumed exclusively radioactive decay. As an example, taking a rock sample and identifying the constituents along with the rate of decay, one can estimate the energy being emitted due to radioactive decay.

(S5) is dilatation dissipation. It represents the loss of energy due to fluctuations in work. This term as well as (S5) are modelled in Section 3.3.

(S6) is the turbulent entropy flux. This term represents the influence of departures from the average entropy flow upon the averaged system; it is a contribution by turbulence. In a physical sense this phenomenon can be imagined as eddies occurring in a water flow. Analogously, swirls in an entropy continuum may be imagined as being represented by this term.

(S7) represents the entropy transfer across the interface. As energy flows from one phase to another, the number of microstates which are energetically possible changes in both states⁵, thus implying a change in entropy [23].

Following a similar process, using that $c'_v = 0$ instead of $T' = 0$, the temperature statement of the energy conservation can be shown to be

$$\begin{aligned}
 \underbrace{c_v \left(\frac{\partial \langle \chi_k \rangle \langle \rho \rangle_\chi \langle T \rangle_\rho}{\partial t} + \nabla \cdot \langle \chi_k \rangle \langle \rho \rangle_\chi \langle \mathbf{v} \rangle_\rho \langle T \rangle_\rho \right)}_{(T1)} &= \underbrace{-\nabla \cdot \langle \chi_k \rangle \langle \mathbf{q} \rangle_\chi}_{(T2)} + \underbrace{\langle \chi_k \rangle \langle Q \rangle_\chi}_{(T3)} + \underbrace{\langle \chi_k \boldsymbol{\tau} \rangle : \nabla \langle \mathbf{v} \rangle_\rho}_{(T4)} \\
 &+ \underbrace{\langle \chi_k \boldsymbol{\tau}'' : \nabla \mathbf{v}'' \rangle}_{(T5)} + \underbrace{\nabla \cdot \langle \chi_k \rho \mathbf{v}'' T'' \rangle}_{(T6)} + \underbrace{\alpha K_T \langle T \rangle_\rho \nabla \cdot \langle \mathbf{v} \rangle_\rho}_{(T7)} \\
 &+ \underbrace{\alpha K_T \langle T \rangle_\rho \nabla \cdot \mathbf{v}''}_{(T8)} + \underbrace{\langle [\rho T (\mathbf{v} - \mathbf{v}_i) - \mathbf{q}] \cdot \nabla \chi_k \rangle}_{(T9)}.
 \end{aligned} \tag{3.30}$$

where from left to right each term represents

⁵referring to the Boltzmann definition of entropy.

(T1) represents the standard Eulerian transport of the averaged temperature.

(T2) - (T5) are identical to (S2) - (S5).

(T6) is a turbulent temperature flux.

(T7) is the averaged expansion caused by isothermal heat flux. When heat enters the system and does not cause a change in temperature, it contributes to expansion work. In this term, $\langle T \rangle_\chi$ is replaced with $\langle T \rangle_\rho$ according to Appendix A.1

(T8) is turbulent isothermal expansion due to heat. This term is neglected; in a relatively continuous system, a field's fluctuations may well be significantly smaller than the averaged values. Additionally, the source of this turbulence term is only a portion of the heat interacting with the system by definition.

(T9) represents the temperature transfer across the interface. As heat flows from one phase to another, the average kinetic energy will change, meaning a change in temperature.

In order to close the system, all terms in Equations (3.29) and (3.30) must be modelled as functions of averaged pressure, temperature and velocity. The following sections are dedicated towards this goal.

3.2 Viscous Stress Tensor

3.2.1 Newtonian Definition

Elasticity (deformation depends only on stress) and plasticity (permanent deformation past a stress limit) are interesting and useful concepts, particularly in geodynamics where the Earth's mantle may be modelled as an elastic solid in the short term and plastic fluid in the long term [24]. However, here the model is restricted to viscosity, resistance to deformation, for simplicity. Following the procedure of Kundu [25], Batchelor [26] and Aris [27] the stress tensor has the form

$$\sigma_{ij} = -\bar{p}\delta_{ij} + \tau_{ij} \quad (3.31)$$

where $-\bar{p}\delta_{ij}$ is the isotropic component and the τ_{ij} is the deviatoric part associated with deformation without any necessary changes in volume. Assuming a linear relation between non-isotropic stress and the velocity gradient $\frac{\partial v_i}{\partial x_j} = \frac{1}{2} \left(\frac{\partial v_i}{\partial x_j} + \frac{\partial v_j}{\partial x_i} \right) + \frac{1}{2} \left(\frac{\partial v_i}{\partial x_j} - \frac{\partial v_j}{\partial x_i} \right)$

$$\tau_{ij} = K_{ijmn}e_{mn} \quad (3.32)$$

where $e_{mn} = \frac{1}{2} \left(\frac{\partial v_m}{\partial x_n} + \frac{\partial v_n}{\partial x_m} \right)$ are the elements of the strain rate tensor and K_{ijmn} is a fourth order tensor coefficient. The antisymmetric part of the velocity gradient tensor $\frac{1}{2} \left(\frac{\partial v_i}{\partial x_j} - \frac{\partial v_j}{\partial x_i} \right)$ is neglected because stresses cannot be generated by rotation (e.g. see [26]). Thus, there is an 81 coefficient relationship between the deviatoric stress and strain rate tensors. If the medium is isotropic, then the stress-strain relation (3.32) has no orientation dependence. Thus, rotations of the coordinate system should not affect K_{ijmn} , implying it is an isotropic tensor. Aris [27, pp 30-34] shows that all isotropic tensors may be expressed linearly in terms of the isotropic second order tensor δ_{ij}

$$K_{ijmn} = \lambda\delta_{ij}\delta_{mn} + \mu\delta_{im}\delta_{jn} + \gamma\delta_{in}\delta_{jm}. \quad (3.33)$$

where λ , μ and γ are constants. It can be shown by conservation of angular momentum that the stress tensor is symmetric ([27, pp 103-105]). Hence, from (3.32), K_{ijmn} is also a symmetric tensor:

$$K_{ijmn} = \lambda\delta_{ij}\delta_{mn} + 2\mu\delta_{im}\delta_{jn}. \quad (3.34)$$

Substituting this into Equation (3.32)

$$\tau_{ij} = K_{ijmn}e_{mn} = 2\mu e_{ij} + \lambda e_{mm}\delta_{ij}. \quad (3.35)$$

Thus the stress tensor (3.31) becomes

$$\sigma_{ij} = -p\delta_{ij} + 2\mu e_{ij} + \lambda e_{mm}\delta_{ij}. \quad (3.36)$$

It is a possible observation that by using Newton's Law of Viscosity (3.32) τ_{ij} , which is idealized as the deviatoric (traceless) component of the stress tensor, has a non-zero trace given by $(2\mu+3\lambda)\nabla \cdot \mathbf{v}$. Because of this, there are two kinds of pressures: mechanical pressure as well as thermodynamic pressure which are equivalent under incompressibility. Mechanical pressure is defined as the mean of the diagonal stresses, i.e. a third of the trace of the stress

tensor $\frac{1}{3}\sigma_{ij}$. If thermodynamic pressure is used, then the trace of τ_{ij} exists separately. To relate the two pressures, set $i = j$ and sum over the three components:

$$\begin{aligned}\sigma_{ii} &= -3p + 2\mu e_{ii} + 3\lambda e_{ii} \\ p &= -\frac{1}{3}\sigma_{ii} + \left(\frac{2}{3}\mu + \lambda\right)\nabla \cdot \mathbf{v}\end{aligned}\tag{3.37}$$

so there is a relation between the two pressures: p , the thermodynamic pressure, and the mechanical pressure $\bar{p} = -\frac{1}{3}\sigma_{ii}$. They are equivalent under the Stokes' assumption $\frac{2}{3}\mu + \lambda = 0$ which is something not taken here. The thermodynamic pressure is that which is used in the equation of state, and if the mean pressure is required it is simple to evaluate it from the relationship

$$\bar{p} - p = -\left(\frac{2}{3}\mu + \lambda\right)\nabla \cdot \mathbf{v}.\tag{3.38}$$

In substituting the above for thermodynamic pressure in (3.36), the stress tensor is split into isotropic (mechanical pressure) and traceless components. The trace is taken out of the strain-rate $2\mu e_{ij}$

$$\sigma_{ij} = -p\delta_{ij} + \xi e_{jj}\delta_{ij} + 2\mu e'_{ij}\tag{3.39}$$

or in vector form

$$\boldsymbol{\sigma} = -p\mathbf{I} + \xi \text{tr}(\boldsymbol{\epsilon})\mathbf{I} + 2\mu\boldsymbol{\epsilon}'.\tag{3.40}$$

where μ is named the shear viscosity, $\xi = \frac{2}{3}\mu + \lambda$ is the bulk viscosity and $e'_{ij} = e_{ij} - \frac{2}{3}\mu e_{ii}$ is the traceless deviatoric strain rate. If mechanical pressure is substituted into equation (3.36) the following results

$$\sigma_{ij} = -\bar{p}\delta_{ij} + 2\mu\epsilon'_{ij}\tag{3.41}$$

where the first term is the isotropic stresses on the system and the second is the traceless stresses.

3.2.2 Averaged Viscous Stress Tensor

In this section the stress equation (3.40) is ensemble averaged, making it suitable for application in the momentum and energy governing equations respectively. A new expression for shear and bulk viscosity coefficients μ and ξ is taken

$$\mu = \frac{\rho}{\langle \rho \rangle_\chi} \mu^* \quad \xi = \frac{\rho}{\langle \rho \rangle_\chi} \xi^*\tag{3.42}$$

where μ^* and ξ^* are assumed to be approximately constant with respect to the ensemble, i.e. $\langle \mu^* \rangle = \mu^*$ and $\langle \xi^* \rangle = \xi^*$. This means that fluctuations in the modified viscosity coefficients are nearly zero within the phases as the experiment is repeated with the same constraints. The strain-rate tensor, which represents deformation of an object, appears throughout the stress tensor (3.40) due to the Newtonian assumption that stress is proportional to strain rate. Thus in preparation to average the stress tensor, the strain rate is averaged

$$\boldsymbol{\epsilon} = \frac{1}{2} \left(\nabla \mathbf{v} + [\nabla \mathbf{v}]^T \right) \quad (3.43)$$

it is required that velocity be mass-weighted when averaged, so taking the weighted averaging (3.2) of the strain rate

$$\langle \boldsymbol{\epsilon} \rangle_\rho = \frac{1}{2 \langle \chi_k \rangle \langle \rho \rangle_\chi} \left(\langle \chi_k \rho \nabla \mathbf{v} \rangle + \langle \chi_k \rho \nabla \mathbf{v} \rangle^T \right) \quad (3.44)$$

before taking the average inside the derivatives, the characteristic function must be taken inside the derivative

$$\begin{aligned} \langle \boldsymbol{\epsilon} \rangle_\rho &= \frac{1}{2 \langle \chi_k \rangle \langle \rho \rangle_\chi} \left(\nabla \langle \chi_k \rho \mathbf{v} \rangle + \nabla \langle \chi_k \rho \mathbf{v} \rangle^T - [\langle \mathbf{v} \nabla \chi_k \rho \rangle + \langle \mathbf{v} \nabla \chi_k \rho \rangle^T] \right) \\ &= \frac{1}{2 \langle \chi_k \rangle \langle \rho \rangle_\chi} \left(\nabla \langle \chi_k \rangle \langle \rho \rangle_\chi \langle \mathbf{v} \rangle_\rho + [\nabla \langle \chi_k \rangle \langle \rho \rangle_\chi \langle \mathbf{v} \rangle_\rho]^T - [\mathbf{U} + \mathbf{U}^T] \right) \end{aligned} \quad (3.45)$$

the term $\mathbf{U} = \langle \mathbf{v} \nabla \chi_k \rho \rangle$ contains information on velocity of masses along the interface. A similar approach to that of Bercovici et al. ([5]) is taken to model this term. Before proceeding it is important to note that their work dealt with averaging the deviatoric stress tensor τ_{ij} while the strain-rate tensor $\boldsymbol{\epsilon}$ is averaged here.

In the compressible case, \mathbf{U} must satisfy the following criteria

1. It must contain an objective component to assure that the stress tensor is objective. Objectivity means that the stress tensor is independent of the reference frame, that is, the motion of the observer.
2. The deviatoric stress tensor $\boldsymbol{\tau}$ must have a zero trace on substitution of the model for \mathbf{U} .
3. \mathbf{U} must not be chosen such that the entire deviatoric stress tensor becomes zero.

4. By the second law of thermodynamics, the dissipation function must be positive definite, i.e. $\nabla \mathbf{v}_k : \tau_k > 0$.

A non-unique solution to these constraints may be chosen

$$\langle \mathbf{U} \rangle = (\nabla \langle \chi_k \rangle \langle \rho \rangle_\chi) \langle \mathbf{v} \rangle_\rho \quad (3.46)$$

the reason for this choice is the reason that, on substituting into Equation (3.45), one obtains

$$\langle \boldsymbol{\epsilon} \rangle_\rho = \frac{1}{2} \left(\nabla \langle \mathbf{v} \rangle_\rho + [\nabla \langle \mathbf{v} \rangle_\rho]^T \right). \quad (3.47)$$

which is analogous to the true strain-rate tensor in Equation 3.43. The strain-rate tensor has been averaged and can be used to average the stress (3.40)

$$\langle \chi_k \sigma \rangle = -\langle \chi_k p \rangle \mathbf{I} + \langle \chi_k \xi \text{tr}(\boldsymbol{\epsilon}) \rangle + \langle 2\chi_k \mu \boldsymbol{\epsilon} \rangle \quad (3.48)$$

substituting (3.42) and using the definition of mass-weighting 3.2 allows the strain-rate averages to be represented as products of averages

$$\begin{aligned} \langle \chi_k \sigma \rangle &= -\langle \chi_k p \rangle \mathbf{I} + \xi^* \langle \chi_k \frac{\rho}{\langle \rho \rangle_\chi} \text{tr}(\boldsymbol{\epsilon}) \rangle + \mu^* \langle 2\chi_k \frac{\rho}{\langle \rho \rangle_\chi} \boldsymbol{\epsilon} \rangle \\ &= -\langle \chi_k p \rangle \mathbf{I} + \xi^* \text{tr} \left(\frac{\langle \chi_k \rho \boldsymbol{\epsilon} \rangle}{\langle \rho \rangle_\chi} \right) + \frac{\mu^*}{\langle \rho \rangle_\chi} \langle 2\chi_k \rho \boldsymbol{\epsilon} \rangle \\ &= -\langle \chi_k p \rangle \mathbf{I} + \xi^* \text{tr}(\langle \chi_k \rangle \langle \boldsymbol{\epsilon} \rangle_\rho) + 2\mu^* \langle \chi_k \rangle \langle \boldsymbol{\epsilon} \rangle_\rho \end{aligned} \quad (3.49)$$

where the interchangeability of trace with average due to linearity has been used. Once again using interchangeability and applying the average of the strain rate tensor shown in Equation (3.47)

$$\begin{aligned} \langle \chi_k \sigma \rangle &= -\langle \chi_k \rangle \langle p \rangle_\chi \mathbf{I} + \xi^* \langle \chi_k \rangle \text{tr} \left(\frac{1}{2} \left(\nabla \langle \mathbf{v} \rangle_\rho + [\nabla \langle \mathbf{v} \rangle_\rho]^T \right) \right) \\ &\quad + \mu^* \langle \chi_k \rangle \left(\nabla \langle \mathbf{v} \rangle_\rho + [\nabla \langle \mathbf{v} \rangle_\rho]^T - 2\nabla \cdot \langle \mathbf{v} \rangle_\rho \right) \end{aligned} \quad (3.50)$$

leading to an averaged expression of stress in terms of variables $\langle p \rangle_\chi$ and $\langle \mathbf{v} \rangle_\rho$

$$\langle \chi_k \sigma \rangle = -\langle \chi_k \rangle \langle p \rangle_\chi \mathbf{I} + \xi^* \langle \chi_k \rangle \nabla \cdot \langle \mathbf{v} \rangle_\rho \mathbf{I} + \mu^* \langle \chi_k \rangle \left(\nabla \langle \mathbf{v} \rangle_\rho + [\nabla \langle \mathbf{v} \rangle_\rho]^T - 2\nabla \cdot \langle \mathbf{v} \rangle_\rho \right) \quad (3.51)$$

3.3 Turbulence Modelling

To close the system, a model must be presented for the turbulence terms - those products of fluctuations that arise from averaging non-linear terms. That is the aim of the following section, where established turbulence models are presented.

3.3.1 Turbulent Stress

The product of fluctuations term $-\langle \chi_k \rho \mathbf{v}'' \mathbf{v}'' \rangle$ is a result of averaging the advection term in Equation (3.13); it is representative of fluctuations in momentum transport. The term can be derived to have the form

$$\langle -\chi_k \rho v_i'' v_j'' \rangle = 2\langle \chi_k \rangle \mu_t \left(\frac{\partial \langle v_i \rangle_\rho}{\partial x_j} + \frac{\partial \langle v_j \rangle_\rho}{\partial x_i} - \frac{1}{3} \frac{\partial \langle v_k \rangle_\rho}{\partial x_k} \delta_{ij} \right) - \frac{1}{3} \langle \chi_k \rho v_i'' v_i'' \rangle. \quad (3.52)$$

by either dimensional analysis [28, p. 47] or the Prandtl mixing length [29, p. 53-60], which is based upon treating turbulent motion as an analogy to molecular diffusion. On referring to Equation (3.37), the above model suggests Reynolds stress is a contribution to the total stress; it enhances the rate of momentum diffusion. Turbulent eddies along the flow act to equalise momentum throughout the system by additional mixing. Along with the above model a new variable is introduced: $\langle \chi_k \rho v_i'' v_i'' \rangle$, however, this contribution may be ignored under the condition $\langle \chi_k \rho v_i'' v_i'' \rangle \ll p$ (see Wilcox [29] and <https://turbmodels.larc.nasa.gov/implementrans.html>). μ_t is a new coefficient, called the *eddy viscosity* which must be assigned to close the system. The eddy viscosity may be approximated, as seen in Monin-Yaglom [15] by

$$\mu_t = l_{mix}^2 \left| \frac{d\langle v \rangle_1}{dx_2} \right| \quad (3.53)$$

where l_{mix} is a mixing length chosen based on the application of the model and depends on a characteristics of the system. For instance, in the flat plate boundary layer mixing-length model, $l_{mix} = \kappa y$ where κ is known as Kármán's constant. Coles and Hirst [30] found that for attached, incompressible boundary layers with and without pressure gradients that $\kappa \approx 0.41$. This is an overly specific case for determining l_{mix} ; more general models are considered in Section 3.3.4.

An important consideration is discussed in the fundamental text by Tennekes and Lumley

([28, p .47]): the equation for Reynolds stress, Equation 3.52), may be nothing more than a dimensional necessity. The correlation coefficient $c_{12} = \frac{\langle v_1 v_2 \rangle}{v'_1 v'_2}$ for turbulent flows driven by shear is of order 1 [28], while the correlation coefficient for molecular motion is of order 10^{-6} , implying the analogy between these kinds of motions is inappropriate, though the dimensions are acceptable. However this expression for turbulent momentum flux is still being applied [31]; an alternative to eddy viscosity seems rare.

3.3.2 Turbulent Scalar Flux

Analogously to Equation (3.52), entropy turbulence is treated as an additional flux of entropy with a coefficient which depends on eddy diffusivity (Monin-Yaglom [15]), Equation 5.9'). This method may be called the gradient diffusion hypothesis [32] and it states that the turbulent transport of a scalar f is related linearly to the mean gradient $\nabla \langle f \rangle$: that the effects of turbulence act to hasten diffusion of scalar f . Thus in the case of entropy

$$\langle \chi_k \rho \mathbf{v}'' s'' \rangle = -K_{s,t} \langle \chi_k \rangle \langle \rho \rangle_\chi \nabla \langle s \rangle_\rho \quad (3.54)$$

where $K_{s,t}$ is the coefficient of turbulent entropy diffusivity. It is related to the eddy viscosity by the turbulent Prandtl number [33]:

$$K_{s,t} = \frac{\mu_t}{Pr_t} \quad (3.55)$$

where Pr_t is between $\cong 0.9$ for near-wall flows and $\cong 0.7$ for free flows [34, p 487]. Similarly, the temperature turbulence term can be treated as an additional quantity down the gradient

$$\langle \chi_k \rho \mathbf{v}'' T'' \rangle = -C_{k,t} \langle \chi_k \rangle \langle \rho \rangle_\chi \nabla \langle T \rangle_\rho \quad (3.56)$$

where $C_{k,t}$ is turbulent conductivity. Note that the above equation, along with Fourier's Heat Law, implies that there is an additional heat flux with coefficient $-C_{k,t}$.

3.3.3 Turbulent Energy Dissipation

The turbulent dissipation rate appears due to non-linearity when the viscous work contributing to the system is averaged. It is a new variable which represents the work energy loss due

to fluctuations in flow acceleration, and must be modelled in order to close the system. It has the form

$$\langle \rho \rangle_\chi e = \langle \chi_k t_{ij} \frac{\partial v_i''}{\partial x_j} \rangle \quad (3.57)$$

where t_{ij} are elements of the viscous stress tensor: $t_{ij} = 2\mu S_{ij} + \xi \frac{\partial v_k}{\partial x_k} \delta_{ij}$. It follows from the turbulent kinetic energy equation (see Wilcox [29]) that

$$\langle \rho \rangle_\chi e = \langle \chi_k t_{ij} \frac{\partial v_i''}{\partial x_j} \rangle = \frac{1}{2} \langle \rho \rangle \langle \chi_k t_{ij} S_{ij}'' \rangle. \quad (3.58)$$

Hence, the equation for turbulent dissipation may be expressed

$$\langle \rho \rangle_\chi e = \langle 2\mu S_{ij} S_{ij}'' + \xi \frac{\partial v_i''}{\partial x_i} \frac{\partial v_i''}{\partial x_i} \rangle \quad (3.59)$$

Assuming the correlation of kinematic shear viscosity ν and bulk viscosity λ with their complement terms is zero

$$\langle \rho \rangle_\chi e = 2\langle \nu \rangle \langle \rho S_{ij}'' S_{ji}'' \rangle + \langle \lambda \rangle \langle \rho \frac{\partial v_i''}{\partial x_i} \frac{\partial v_i''}{\partial x_i} \rangle \quad (3.60)$$

splitting S_{ij} into vorticity and deformation

$$\langle \rho \rangle_\chi e = \langle \nu \rangle \left(\langle \rho \omega_i \omega_i'' \rangle + \langle \rho \frac{\partial v_i''}{\partial x_j} \frac{\partial v_j''}{\partial x_i} \rangle \right) + \langle \lambda \rangle \langle \rho \frac{\partial v_i''}{\partial x_i} \frac{\partial v_i''}{\partial x_i} \rangle \quad (3.61)$$

assuming that the turbulence is homogeneous, meaning that the turbulent flow is uniform in all directions⁶, one can replace $\frac{\partial v_i''}{\partial x_j} \frac{\partial v_j''}{\partial x_i} \approx \left(\frac{\partial v_i''}{\partial x_i} \right)^2$

$$\langle \rho \rangle_\chi e = \langle \rho \rangle_\chi e_s + \langle \rho \rangle_\chi e_d + \langle \rho \rangle_\chi e_b \quad (3.62)$$

where $\langle \rho \rangle_\chi e_s = \langle \nu \rangle \langle \rho \omega_i'' \omega_i'' \rangle$ is known as the solenoidal dissipation; $\langle \rho \rangle_\chi e_d = 2\langle \nu \rangle \langle \rho \frac{\partial v_i}{\partial x_i} \frac{\partial v_i}{\partial x_i} \rangle$ as the dilatation dissipation and $\langle \rho \rangle_\chi e_b = \langle \lambda \rangle \langle \rho \frac{\partial v_i}{\partial x_i} \frac{\partial v_i}{\partial x_i} \rangle$ as the bulk (dilatation) dissipation.

Sarkar et al.[35][36] proposes an algebraic model relating the solenoidal dissipation e_s and dilatation and bulk dissipation e_d .

$$e_d = \alpha_1 e_s M_t^2 \quad (3.63)$$

$$e_b = \alpha_2 e_s M_t^2 \quad (3.64)$$

⁶that is, the probability of the flow being excited in any direction has a uniform distribution

where M_t is the turbulent Mach number defined by $M_t = \sqrt{q^2/\gamma R\langle T \rangle_\chi}$. Hence the model for e becomes

$$e = e_s (1 + (\alpha_1 + \alpha_2)e_s M_t^2) \quad (3.65)$$

replacing the variable e with e_s . An equation of transport for e_s may be used to complete the system. A transport equation that may be used is a multiphase analogy of the dissipation rate equation of Sarkar (details can be found with Wilcox [29], Sarkar [35], Sarkar-Lakshmanan [36] and Launder [37]) with phase interaction terms that may be modelled by method of Simonin-Viollet [38] or Troshko-Hassan [39]

$$\begin{aligned} \frac{\partial \langle \chi_k \rangle \langle \rho \rangle_\chi e_{s,k}}{\partial t} + \nabla \cdot (\langle \chi_k \rangle \langle \rho \rangle_\chi \langle \mathbf{v} \rangle_\rho e_{s,k}) = & \nabla \cdot \left(\langle \chi_k \rangle \left(\mu + \frac{\mu_t}{\sigma_k} \right) \nabla e_{s,k} \right) + \langle \chi_k \rangle (C_{1e} \langle \boldsymbol{\tau} \rangle_\chi : \nabla \langle \mathbf{v} \rangle_{\rho_k} - \\ & C_{2e} \langle \rho \rangle_\chi e_s) + \sum_z^N K_{k,z} (C_{k,z} e_{s,z} - C_{z,k} e_{s,k}) - \sum_{z=1}^N K_{z,k} (\langle \mathbf{v} \rangle_{\rho_z} - \\ & \langle \mathbf{v} \rangle_{\rho_k}) \frac{\mu_{t,z}}{\langle \chi_z \rangle \sigma_z} \nabla \langle \chi_z \rangle + \sum_{z=1}^N K_{z,k} (\langle \mathbf{v} \rangle_{\rho_z} - \langle \mathbf{v} \rangle_{\rho_k}) \frac{\mu_{t,k}}{\langle \chi_k \rangle \sigma_k} \nabla \langle \chi_k \rangle + \Pi_{e_s,k} \end{aligned} \quad (3.66)$$

where $e_{s,k}$ is the solenoidal dissipation in the k 'th phase and $k = \langle \chi_k \rho v_i'' v_i'' \rangle$ is the turbulent kinetic energy. Terms on the left-hand side represent the sum of the local and advective changes in dilatation dissipation. On the right-hand side, the terms represent viscous diffusion, dissipation, dispersion and a set of three inter-phase exchange respectively, with coefficients of the form $K_{k,k}$ and $C_{k,k}$. To complete the system, a transport equation is required for the turbulent kinetic energy k_k . Wilcox provides the one-phase transport equation in his statement of the $k - \epsilon$ model, which may be presented in multi-phase form

$$\begin{aligned} \frac{\partial \langle \chi_k \rangle \langle \rho \rangle_\chi k}{\partial t} + \nabla \cdot (\langle \chi_k \rangle \langle \rho \rangle_\chi \langle \mathbf{v} \rangle_\rho k_k) = & \nabla \cdot \left(\langle \chi_k \rangle \left(\mu + \frac{\mu_t}{\sigma_k} \right) \nabla k_k \right) + (\langle \chi_k \rangle \langle \boldsymbol{\tau} \rangle : \nabla \langle \mathbf{v} \rangle - \langle \chi_k \rangle \langle \rho \rangle_\chi e_s) \\ & + \sum_z^N K_{k,z} (C_{k,z} k_z - C_{z,k} k_k) - \sum_{z=1}^N K_{z,k} (\langle \mathbf{v} \rangle_{\rho_z} - \langle \mathbf{v} \rangle_{\rho_k}) \frac{\mu_{t,z}}{\langle \chi_z \rangle \sigma_z} \nabla \langle \chi_z \rangle \\ & + \sum_{z=1}^N K_{z,k} (\langle \mathbf{v} \rangle_{\rho_z} - \langle \mathbf{v} \rangle_{\rho_k}) \frac{\mu_{t,k}}{\langle \chi_k \rangle \sigma_k} \nabla \langle \chi_k \rangle + \Pi_{k_z}. \end{aligned} \quad (3.67)$$

Because in Equation (3.66) there is an additional variable of k_k , the turbulent kinetic energy must also modelled to close the system. Hence, in Equation (3.52) the kinetic energy term

may be kept. On the other hand, if dilatation dissipation is ignored as it usually is in zero-equation models [29, p 250], the kinetic energy may be neglected also, leading to a much simpler system without two additional transport equations.

3.3.4 Comparison of Turbulence Models

To close the system one has to incorporate a model for the turbulence terms⁷ which arise as a by-product of the averaging process: in the case of this document, turbulent dilatation dissipation; entropy, temperature and momentum flux. The simplest category of turbulence models consists of the zero-, one- and two-equation models. The name of these models indicate the number of additional transport equations that are implemented. The zero-equation models are thus simplest to implement, but of course, at a price of accuracy and rigour; for instance, turbulent dilatation dissipation and kinetic energy are neglected entirely in zero-equation models.

Zero-Equation models

These models are designed for eddy viscosity alone, allowing inclusion of terms described in Sections 3.3.1-3.3.2 - turbulent dilatation dissipation is neglected in this case. An old, yet robust, model of this type is the *Cebeci-Smith* model [40]. It describes the flow in two layers: one close to the edge of the flow, which must be specified, where surface stresses have a larger impact and the second layer is of the remaining fluid (see Figure 3.2).) The *Baldwin-Lomax* model [41] is similar in that it splits the flow into two layers, but it does not require the determination of the flow edge and is less accurate at modelling separated flow [42]. These models are considered robust, giving non-physical results only in unusual cases [43].

One-Equation models

The Spalart-Allmaras model [44] is another option to solve for eddy viscosity. It presents a transport equation for a variable directly related to it. Recall transport equations generally have, on the left-hand side, the material transport rate of the physical parameter, and on

⁷for application in code, https://www.cfd-online.com/Wiki/RANS-based_turbulence_models is a useful resource.

the right-hand side: sources of production, diffusive transport, etc. This approach is aimed at boundary layer, pipe or channel flows in aeronautical applications.

Two-Equation models

Instead of the one transport equation model, two equations may be used; one to solve for turbulent kinetic energy (Equation (3.67)) and one to solve for either turbulent dilatation (Equation 3.66) or specific (ω) dissipation [37]. An advantage of these models is that, by the nature of transport equations, the modelled turbulence has memory. That is, effects such as diffusion of turbulent energy exist (unlike in the zero- and one- equation models).

Summary

With the inclusion of multiple phases, the one- and two-equation models become significantly more complicated, as the transport equations introduced have interfacial terms, which must be also modelled. Modelling of turbulent interfacial interaction is a bit beyond the scope of this study, thus, in Chapter 4, a zero-equation model for eddy viscosity will be used, where turbulent dissipation and kinetic energy are ignored⁸. The nature of the Prandtl molecular diffusion analogy means that these models are only applicable for dimensions higher than 1. Due to time/page restrictions a simpler model for eddy viscosity is proposed for 1D applications

$$\mu^* = \mu \times 10^{\gamma f} \quad (3.68)$$

⁸If using two-equation turbulence it may be worthwhile to include kinetic energy balance into the governing equations, as its turbulent portion is being modelled anyway.

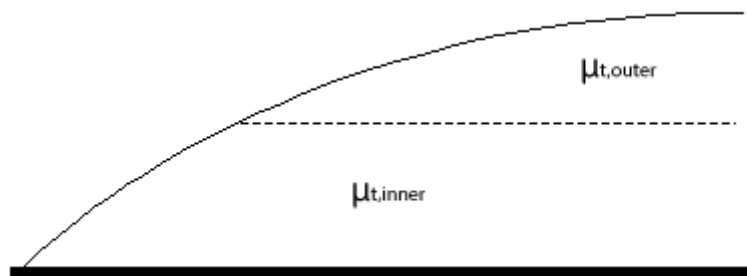


FIGURE 3.2: Illustration of a flat-plate the boundary layer problem. $\mu_{t,inner}$ is different to $\mu_{t,outer}$ due to the greater effects of stress near the solid plate. In zero-equation models, the inner and outer turbulent viscosity are equal.

where γ is a constant, and $f = |\frac{dv_y}{dy}|/|\frac{dv_y}{dy}|_{max}$. The above law magnifies μ up to γ orders of magnitude to simulate the addition of turbulent eddies enhancing mixing. This particular f is used as a compression analogy to the gradients in the higher dimensional turbulence model for eddy viscosity.

3.4 Interfacial Interactions

Interactions across phase boundaries must be modelled to close the system. Rather than incorporating specific boundary conditions for each experiment, generic interfacial transport models may be used because the system is averaged.

3.4.1 Interfacial Momentum Transport

The last unknown in the momentum equation (??) to deal with is the term labelled (M6). This term represents the momentum transfer due to the presence of other phases. The model taken [5] is

$$\langle \rho \mathbf{v} [(\mathbf{v} - \mathbf{v}_i) - \sigma] \cdot \nabla \chi_k \rangle = \sum_{z \neq k} c_{k,z} (\mathbf{v}_k - \mathbf{v}_z) + p_w \nabla \cdot \langle \chi_k \rangle + \omega_k \nabla (\sigma \alpha). \quad (3.69)$$

where $\mathbf{v}_k = \frac{\langle \chi_k \rho \mathbf{v} \rangle}{\langle \chi_k \rangle \langle \rho \rangle_\chi}$ as introduced in Equations 3.3 and 3.4. The first two terms on the right-hand side represent a Galilean invariant phase-interaction forces; drag, where the momentum of the medium may act directly against the particle, and lift, where non-uniform momentum in the medium may induce a moment in the projectile. Galilean invariance means that no matter what reference frame is used to observe the system, the absolute forces are the same. Newton's laws of motion hold between all frames.

Each of the new objects $c_{k,z}$, p_w and ω_k must be expanded on. The term $c_{k,z} (\mathbf{v}_k - \mathbf{v}_z)$ comes from balance of viscous forces per volume at the interface and has dimensionality $\frac{m}{l^2 t^2}$ where m is mass, l is length and t is time. Forces per volume on either side of the interface must depend on viscosity $\mu_k \sim \frac{m}{lt}$, some characteristic length $\delta_k \sim l$ and velocities $\mathbf{v}_i \sim \frac{l}{t}$ and $\mathbf{v}_k \sim \frac{l}{t}$, where i represents interface property and k represents a phase property. Considering the dimensionality of the viscous forces, and assuming that they match at the

interface between two phases (Newton's Third Law) one has

$$\mu_1 \frac{\mathbf{v}_1 - \mathbf{v}_i}{\delta_1^2} = \mu_2 \frac{\mathbf{v}_i - \mathbf{v}_2}{\delta_2^2} \quad (3.70)$$

solving for \mathbf{v}_i

$$\mathbf{v}_i = \frac{\mu_1 \mu_2 (\mathbf{v}_1 - \mathbf{v}_2)}{\mu_2 \delta_1^2 + \mu_1 \delta_2^2} \quad (3.71)$$

and back-substituting into either side gives the equation for viscous forces across the interface

$$c_{1,2} (\mathbf{v}_k - \mathbf{v}_z) = \frac{\mu_1 \mu_2 (\mathbf{v}_1 - \mathbf{v}_2)}{\mu_2 \delta_1^2 + \mu_1 \delta_2^2} \quad (3.72)$$

hence the general expression $c_{1,2} = \frac{\mu_1 \mu_2}{\mu_2 \delta_1^2 + \mu_1 \delta_2^2}$ can be taken. Lastly, δ_1 and δ_2 must be modelled. Assume that they are related to permeability i.e. capacity for material to transmit fluid, such that they are functions of only the phase fraction: $\delta_k = \langle \chi_k \rangle \delta$ where δ is some characteristic length independent of phase. McKenzie [1] shows, assuming Darcy's Law, that $c_{k,z} = \frac{\mu \langle \chi_k \rangle}{K_\chi}$ where K_χ is the permeability of the k 'th phase. If $\frac{\mu_2}{\mu_1} \rightarrow 0$, Darcy's Law should hold in the above case also. Hence,

$$\lim_{\frac{\mu_2}{\mu_1} \rightarrow 0} c = \lim_{\frac{\mu_2}{\mu_1} \rightarrow 0} \frac{\mu_1 \mu_2}{\mu_2 \delta_1^2 + \mu_1 \delta_2^2} = \frac{\mu_2}{\delta_2^2} \quad (3.73)$$

but Darcy's law shows

$$\lim_{\frac{\mu_2}{\mu_1} \rightarrow 0} c = \frac{\mu_2}{\delta_2^2} = \frac{\mu_2 \langle \chi_2 \rangle}{K_{\chi_2}} \quad (3.74)$$

Hence, $\delta_2 = \frac{\sqrt{K_{\chi_2}}}{\langle \chi_2 \rangle}$. Assuming material invariance, $\delta_k = \frac{\sqrt{K_\chi}}{\langle \chi_k \rangle}$. Hence,

$$c = \frac{\mu_1 \mu_2}{\mu_2 \frac{K_{\chi_1}}{\langle \chi_1 \rangle} + \mu_1 \frac{K_{\chi_2}}{\langle \chi_2 \rangle}}. \quad (3.75)$$

This equation is postulated to extend up to n phases like so

$$c = \frac{\prod_i^n \mu_i}{\sum_i^n \mu_i \left[\sum_{j \neq i}^n \frac{K_{\chi_j}}{\langle \chi_j \rangle} \right]} \quad (3.76)$$

though a further study is required. Permeability dependence of K_χ on the phase fraction $\langle \chi_k \rangle$ has been empirically accepted in the case of a two-phase system $k \in \{m, f\}$ where $\mu_m \gg \mu_f$ to have the form $K_\chi = k_0 \langle \chi_k \rangle^m$ with $2 \leq m \leq 3$. Clearly this is not the arbitrary

multi-phase case, but for now it is an acceptable model.

The last term on the right-hand side of (3.69) is the surface tension term. It is a result of an energy anomaly in the interface between phases due to the imbalance of intramolecular forces. The larger the activation energy (i.e. bond strength) of particles in phase k , the larger the anomaly is at the interface. The Eyring model of viscosity claims that μ is related exponentially to activation energy (Bird et al. [45]). Hence, the partitioning of surface energy between the phases containing components of different activation energy depends on μ . An adapted model from that proposed by Bercovici and Ricard [8]) is the following

$$\omega_k = \frac{\langle \chi_k \rangle \mu_k}{\sum_i \langle \chi_i \rangle \mu_i} \quad (3.77)$$

The interfacial pressure term p_ω can be modelled as follows

$$p_\omega = \sum_k \frac{1 - \omega_k}{\sum_i (1 - \omega_i)} \langle p \rangle_\chi. \quad (3.78)$$

An example of the above equation is presented by considering the pressure difference across the interface in a three-component mixture of phases 1, 2 and 3. In the case where viscosity of phase 1 is dominant, implying by (3.77) that the surface energy (and the selvedge) is embedded in phase 1 and $\omega_1 = 1$, $\omega_2 = \omega_3 = 0$; the total pressure difference across the interface is approximated by $\Delta p_{12} \approx (p_1 - p_\omega)$ with $(p_2 - p_\omega) \approx 0$ and $(p_3 - p_\omega) \approx 0$. As predicted by (3.78), $p_\omega = \frac{1}{2}(p_2 + p_3)$.

On combining the four equations (3.51), (??), (3.52) and (3.69) the conservation of momentum equation becomes

$$\begin{aligned} \frac{\partial \langle \chi_k \rangle \langle \rho \rangle_\chi \langle \mathbf{v} \rangle_\rho}{\partial t} + \nabla \cdot \langle \chi_k \rangle \langle \rho \rangle_\chi \langle \mathbf{v} \rangle_\rho \langle \mathbf{v} \rangle_\rho = \\ = \nabla \cdot \left[-\langle \chi_k \rangle \langle p \rangle_\chi \mathbf{I} + \xi^* \langle \chi_k \rangle \nabla \cdot \langle \mathbf{v} \rangle_\rho \mathbf{I} + (\mu^* - 2\mu_t) \langle \chi_k \rangle \left(\nabla \langle \mathbf{v} \rangle_\rho + (\nabla \langle \mathbf{v} \rangle_\rho)^T \right) \right. \\ \left. + \frac{2\langle \chi_k \rangle \mu_t}{3} \nabla \cdot \langle \mathbf{v} \rangle_\rho \mathbf{I} \right] + \langle \chi_k \rangle \langle \rho \rangle_\chi \langle \mathbf{b} \rangle_\rho - \sum_{z \neq k} c_{k,z} \left(\frac{\langle \chi_k \rho \mathbf{v} \rangle}{\langle \chi_k \rangle \langle \rho \rangle_\chi} - \frac{\langle \chi_z \rho \mathbf{v} \rangle}{\langle \chi_z \rangle \langle \rho \rangle_\chi} \right) \\ + p_\omega \nabla \cdot \langle \chi_k \rangle + \frac{\langle \chi_k \rangle \mu_k}{\sum_i \langle \chi_i \rangle \mu_i} \nabla(\sigma\alpha) \end{aligned} \quad (3.79)$$

3.4.2 Interfacial Energy Transport

Two-phase interfacial energy transport can be neglected by assuming thermal equilibrium - that the phases have the same temperature - and taking the difference in the temperature equations; indeed, this is what is done in the examples section of this thesis. Because of thermal equilibrium, the amount of temperature leaving one phase must equal the temperature leaving the other phase. Coming up with a model for general multi-phase entropy and temperature interfacial transport is still a problem, though Oliveira et al. [11] has proposed a transport equation for interfacial internal energy transport.

3.5 Additional Laws

3.5.1 Murnaghan's Equation of State

Although the ideal gas law may be used throughout aerodynamics and is very easy to deal with, it is inapplicable in areas of geodynamics where high pressures can exist. A more appropriate equation of state is the Murnaghan's Equation of State ⁹. It follows from a linear expansion in the definition of permeability. Murnaghan's equation of state is

$$p = \frac{K_0}{K'_0} \left[\left(\frac{\rho}{\rho_0} \right)^{-K'_0} - 1 \right] \quad (3.80)$$

where K_0 is bulk modulus, K'_0 is the derivative of the bulk modulus with respect to pressure and ρ_0 is initial density before some compression or expansion. Even if it is assumed that the average of K_0 , K'_0 and ρ_0 is independent of the realization, it is difficult to express Murnaghan's Law in terms of averaged variables due to the power on the right-hand side. In dealing with the quadratic term in the transport equations, one can apply a Reynolds Expansion treatment. However, $-K'_0$ cannot be treated in the same way. Instead, a revised Murnaghan's Law is used: assume that the following holds for averaged variables for a different parameter K_0^*

$$K_0^* = \langle \rho \rangle_x \left(\frac{\partial \langle p \rangle_x}{\partial \langle \rho \rangle_\rho} \right)_T \quad (3.81)$$

⁹At pressures pertaining to the mantle transition zone and lower mantle, other EoS should be used (e.g. Vinet [46]).

then taking a revised Murnaghan's assumption that K_0^* is a linear function of averaged pressure

$$K_0^* = K_0^* + \langle p \rangle_\chi \frac{\partial K_0^*}{\partial \langle p \rangle_\chi} \quad (3.82)$$

then on solving Equation (3.81)

$$\langle p \rangle_\chi = K_0^*/K_0^{*'} \left[\left(\frac{\langle \rho \rangle_\chi}{\langle \rho \rangle_0} \right)^{-K_0^{*'}} - 1 \right] \quad (3.83)$$

now assuming K_0^* and K_0 are approximately equal, the following can be taken

$$\langle p \rangle_\chi = K_0/K_0' \left[\left(\frac{\langle \rho \rangle_\chi}{\langle \rho \rangle_0} \right)^{-K_0'} - 1 \right] \quad (3.84)$$

this process in the end has the same meaning as stating that Murnaghan's equation of state holds identically for averaged variables.

3.5.2 Averaged Heat Flux

Heat flux \mathbf{q} can be envisioned to increase as absolute temperature gradient increases; the flux of heat increases with the temperature disparity between the hot sources and colder sinks. The statement of Fourier's heat conduction law is that local heat flux density is linearly proportional to the negative temperature gradient

$$\mathbf{q} = -K \nabla T \quad (3.85)$$

and after averaging while assuming the temperature T is not realization-dependent, as in Equation (3.25)

$$\langle \chi_k \rangle \langle \mathbf{q} \rangle_\chi = -C_k \langle \chi_k \rangle \nabla T \quad (3.86)$$

C_k is the k 'th phase's conductivity and will be taken as a constant with respect to phases. If T depends on realization, as in the temperature energy Equation (3.30), another assumption must be taken. Since T is mass-weighted in Equation (3.30), while it is phase-weighted in Fourier's law. Taking the phase-weighted expansion of temperature in Fourier's law

$$\langle \chi_k \rangle \langle \mathbf{q} \rangle_\chi = -C_k \langle \chi_k \rangle \nabla \langle T \rangle_\chi + \langle C_k \chi_k \nabla T'' \rangle \quad (3.87)$$

notice that for phase-weighted ∇T , $\langle \chi_k \rangle \langle \nabla T'' \rangle_\chi = 0$. First see the Reynolds expansion

$$\nabla T = \langle \nabla T \rangle_\chi + (\nabla T)'' \quad (3.88)$$

now splitting the phases and averaging

$$\langle \chi_k \nabla T \rangle_\chi = \langle \chi_k \rangle \langle \nabla T \rangle_\chi + \langle \chi_k (\nabla T)'' \rangle \quad (3.89)$$

it follows from the definition of the phase average of ∇T

$$\langle \chi_k (\nabla T)'' \rangle = 0. \quad (3.90)$$

A question arises: under what conditions may it be assumed $\langle \chi_k \nabla T'' \rangle \approx \langle \chi_k (\nabla T)'' \rangle$? Taking the phase-weighted Reynolds expansion of both T and ∇T .

$$\begin{aligned} T &= \langle T \rangle_\chi + T' \\ \nabla T &= \langle \nabla T \rangle_\chi + (\nabla T)'' \end{aligned}$$

Taking the gradient on the first equation

$$\nabla T = \nabla \langle T \rangle_\chi + \nabla T' \quad (3.91)$$

then subtracting from the second equation

$$[\langle \nabla T \rangle_\chi - \nabla \langle T \rangle_\chi] + [(\nabla T)'' - \nabla (T')] = 0 \quad (3.92)$$

Hence, $\langle \chi_k \nabla T'' \rangle \approx \langle \chi_k (\nabla T)'' \rangle$ if

$$\langle \nabla T \rangle_\chi \approx \nabla \langle T \rangle_\chi. \quad (3.93)$$

In the case of the un-weighted average, this is true as long as T is a well-defined function. However it the above does not hold in general for phase-weighting:

$$\frac{\langle \chi_k \nabla f \rangle}{\langle \chi_k \rangle} \neq \nabla \frac{\langle \chi_k f \rangle}{\langle \chi_k \rangle} \quad (3.94)$$

for an arbitrary function f . In the interest of proceeding using Fourier's Heat Law for the temperature equation, the assumption that $\langle \nabla T \rangle_\chi \approx \nabla \langle T \rangle_\chi$ is taken. One more issue with Equation (3.87) is that T is phase-weighted, whereas in Equation 3.30 it is mass-weighted.

As long as the ratio $\frac{\overline{\chi_k \rho' T'}}{\chi_k \bar{\rho}}$ is negligible, the mass- and phase-weightings may be interchanged (see Appendix (A.1)). Thus, taking $\langle \nabla T \rangle_\chi \approx \nabla \langle T \rangle_\chi$ and $\langle T \rangle_\chi \approx \langle T \rangle_\rho$, Fourier's Law takes the expression

$$\langle \chi_k \rangle \langle \mathbf{q} \rangle_\chi = -C_k \langle \chi_k \rangle \nabla \langle T \rangle_\rho \quad (3.95)$$

using the above in conjunction with Equation (3.84) allows the system of Equations (3.30) or (3.29); (3.17) and (3.2) to be complete.

3.5.3 Pressure Difference

One final constitutive law is required for the closure of the system: an expression for the pressure difference between phases. This equation has been studied as a part of many modelling schemes, e.g. McKenzie's two-phase Darcy flow [1], Bercovici and Ricard's material invariant two-phase flow with surface tension [8] for which Šramek provided additional thermodynamic rigour [9]. The viscous equivalent of the visco-elastic plastic equation proposed by Oliveira et al. [11] is applied here, i.e.

$$\Delta P_{k,j} = -\xi (\omega_k \phi_k \nabla \cdot \mathbf{v}_k - \omega_j \phi_j \nabla \cdot \mathbf{v}_j) \quad (3.96)$$

where $\Delta P_{k,j} = P_k - P_j$.

3.6 Summary

Combining Equations (3.9), (3.79) and (3.30) or (3.29) with the models of Sections 3.2-3.5, a complete system of compressible n -phase m -component equations with phase-specific variables of $\langle \chi_k \rangle$, $\langle \rho_k \rangle_\chi$, $\langle \mathbf{v} \rangle_\rho$, $\langle p \rangle_\chi$ and either $\langle T \rangle_\rho$ or $\langle s \rangle_\rho$ is formed. Though the turbulence and interface interactions models may be simple, they are ideally robust enough for analysis in the following chapter.

4

Examples

In this section, some simple, yet illustrative, numerical examples are presented that highlight some of the potential uses of our system of equations for general cases of partial melting. I explore the behaviour of a thermally-driven upwelling experiencing partial decompression melting, under three different working hypothesis:

- Non-turbulent formulation with incompressible phases $\frac{D\rho}{Dt} = 0$
- Turbulent formulation with incompressible phases $\frac{D\rho}{Dt} = 0$
- Non-turbulent formulation with compressible phases

To keep the analysis tractable and focus on the major features of the model, we restrict ourselves to the illustrative case of systems made up entirely of olivine (i.e. a single solid solution with two end-members Mg_2SiO_4 and Fe_2SiO_4 ; the melt phase has the same end-members). Thus three chemical components are kept track of, namely, FeO , MgO and SiO_2 .

Thermodynamic data comes from the internally-consistent database of [47]. In addition, I solve the quasi-static Navier-Stokes equation (i.e. $\frac{\partial \phi_k \rho_k \mathbf{v}_k}{\partial t} = 0$). Mass-transfers rates (i.e. Γ_m, Γ_b), solutions from the Murnaghan EoS (Equation 3.84), and physical properties (e.g. ρ_k, c_p) are consistently retrieved from the thermodynamic solver. More information on the thermodynamic solver can be found in Oliveira et al. [11].

The work in the following chapter may be extended by including an extended thermodynamic database as well as 2D case studies. A number of benchmarks used to validate the numerical scheme are presented in Appendix B, Oliveira et al. [11].

4.1 Model description

This example solves a transient two-phase (solid (s) - fluid (f)) multi-component reactive transport problem for the simple 1D case of a viscous olivine solid solution with homogeneous initial composition. The experiment is run over a 200 km deep column discretized with 401 nodes and 2.000 randomly distributed Lagrangian markers (~ 5 particles per element) and for 2.5 Ma. The main model features are: (1) uniform initial bulk composition of $\text{Mg\#} = 0.5$, (2) constant viscosities ($\mu_s = 10^{20}$ Pa s and $\mu_f = 1$ Pa s and $\xi = \mu$) (3) viscous interaction coefficient $c_{s,f} = 1/k_0$, where $k_0 = 10^{-11}$ Pa s is the permeability constant, (4) constant mantle inflow at the bottom of the domain, $\mathbf{v}_s = v_s^{in}$, (5) fixed temperature $T_{bot} = 1920\text{K}$, composition c_{in}^b and zero melt fraction at the bottom (inflow) of the domain, (6) melt is freely allowed to flow out of the upper part of the domain, (7) the solid pressure is fixed in the bottom boundary and (8) initial temperature field with a thermal anomaly given by,

$$\begin{aligned}
 T(y) &= T_{ref} + 75 [1 + \cos(\pi \min\{r(y); 1\})] \\
 \text{where, } r(x, y) &= 1.5 \sqrt{\left(\frac{x}{2 \times 10^5}\right)^2 + \left(\frac{y - 70 \times 10^5}{10^5}\right)^2} \\
 T_{ref} &= m (y - 2 \times 10^5) + T_{bot} \\
 T_{bot} &= 1920 \\
 m &= 3 \times 10^5
 \end{aligned} \tag{4.1}$$

Since the examples are of 1D compaction/expansion, the model for eddy viscosity proposed in Equation 3.68 will be used, i.e.

$$\mu^* = \mu \times 10^{\gamma f} \quad (4.2)$$

where γ is a constant, and $f = |\frac{dv_y}{dy}|/|\frac{dv_y}{dy}|_{max}$. The above law magnifies μ up to γ orders of magnitude to simulate the addition of turbulent eddies enhancing mixing.

4.2 Results

The transient nature of the problem is illustrated using a unified colour scale in all the figures, where blue = initial time, and red = final time. Because of the imposed material inflow at the bottom of the numerical domain, the initially melt-free system is advected upwards. Figures 4.1 to 4.6 illustrate the behaviour of our system, where the y-axis corresponds to height in meters.

4.2.1 Non-turbulent and incompressible formulation

Figure 4.1 presents the predicted non-turbulent, incompressible evolution of the olivine system from a depth of 200km. At time $t = 0$, Figure 4.1D shows that melting begins around the height of 50km, where the temperature is about 2000K. Partial melting causes a drop in the FeO content of the solid phase, which is reflected in a higher Mg# number and an associated decrease in density. As expected for this binary system, the opposite behavior (FeO enrichment) may be observed in the melt phase. T, #Mg and ϕ increases to a local maximum around 130km. Higher than that, the melt ratio begins to decrease as reduced temperatures limit the amount of melting. As $t > 0$, the thermal instability travels upwards (due to the bottom inflow), enters lower pressure zones and causes decompression melting.

In Figure 4.2, the development of densities (plots labelled A and B), velocities (C and D) and pressures (E) are illustrated. The density of the solid begins at 4000kg/m³, and decreases in presence of melt due to its lower content in FeO. At $t = 0$, the solid velocity steadily decreases with height with the melt fraction. The eventual overtaking of the solid velocity by melt velocity is due to lower density of ρ_f causing the fluid to experience less gravitational

pull. As time progresses, however, the density difference plot shows that the fluid density can outweigh the solid density, and thus the velocity difference become smaller. The relative pressure of the fluid (stronger fluid's overpressure, i.e. compaction) is a maximum, where the solid density is minimum, as the increased solid's volume pushes against the melt.

4.2.2 Turbulent and incompressible formulation

The thermal, compositional and melt evolution is similar to the previous case, and thus it is not shown here. However, Figures 4.3-4.4 show the influence of the turbulence model on velocities and pressure difference for different values of γ . In general, the bigger γ is, the more momentum diffusion is enhanced by the turbulent effect. In velocity, Figure 4.3, this causes the gradients to become more extreme as accelerations are dampened; it also means the velocity magnitudes are smaller than in the non-turbulent case. When $\gamma = 1$, the effect of the eddy viscosity makes the pressure differences bigger (Figure 4.4A) - possibly due to the increased pressure because of the slower-moving system. The new viscosity is not homogeneous throughout the column (as it depends on the velocity gradient), which is why the curve shows a different pattern to the non-turbulent case. When γ is increased to 2 (Figure 4.4B), the eddy viscosity changes by an additional order of magnitude, causing a further increase of the pressure difference (Figure 4.4) and a further decrease in velocity differences (Figure 4.3C and D).

4.2.3 Compressible formulation

In Figure 4.5, the temperature in the compressible case is not noticeably different from the incompressible case, which implies that the thermal expansivity is small and that the overall advection of the system is similar in both cases. The phase abundance in subfigure B follows a similar evolution as the incompressible case in Figure 4.1D.

Figure 4.6C, however, shows a different solid velocity behavior; the curve has a much larger amplitude changes with time in an irregular fashion compared to the incompressible case (Figure 4.2C). The (mass-weighted) velocity derivatives in the model are all different and the inclusion of additional terms in the mass conservation equation (i.e. in this case

$\frac{D\rho}{Dt} \neq 0$) cause this alteration. Consequently, the pressure difference undergoes a significant change, whereas the velocity difference remains the same. This suggests that the incorporation of compressibility affects the velocity patterns - causing overpressure of the fluid; the velocity changes are however controlled by the interaction terms, which in this case remain unchanged. At lower depths, the relative fluid pressure is much higher. That the fluid may contract is clear from the second panel, where fluid density eventually overtakes solid density. The pressure on the solid transfers to the fluid by making it compact further, thus giving the Figure 4.6E.

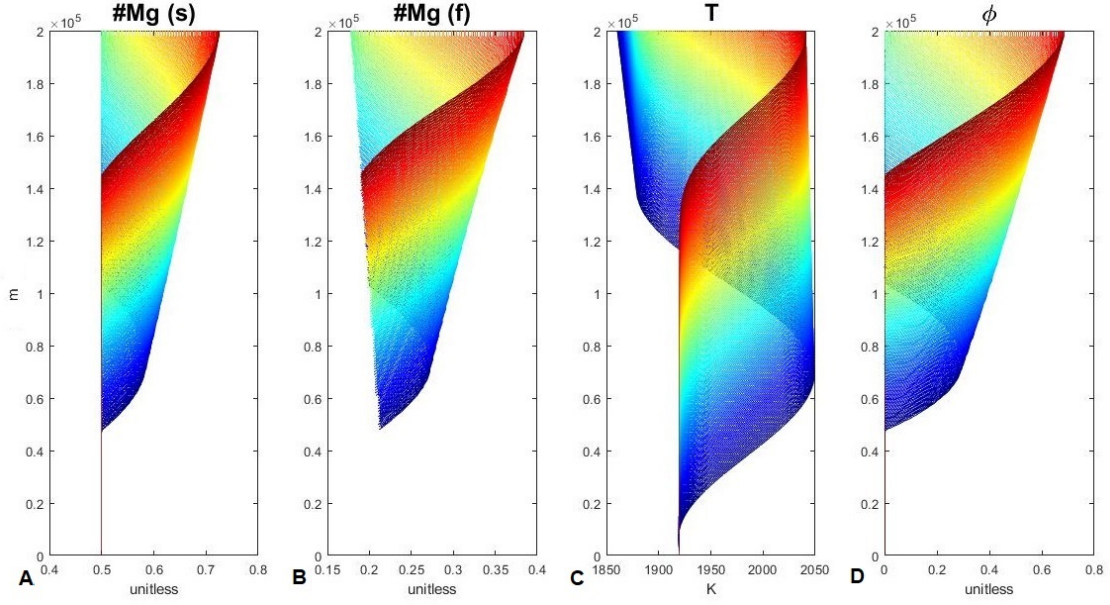


FIGURE 4.1: Incompressible non-turbulent evolution with depth of fluid variables, particularly, (A) $\#Mg$ in the solid, (B) $\#Mg$ in the liquid, (C) temperature and (D) phase abundance. The plot is colour-coded from blue, indicating initial time, to red, indicating final time. For instance, as time progresses, $\#Mg$ increases in the solid and liquid while it travels upward

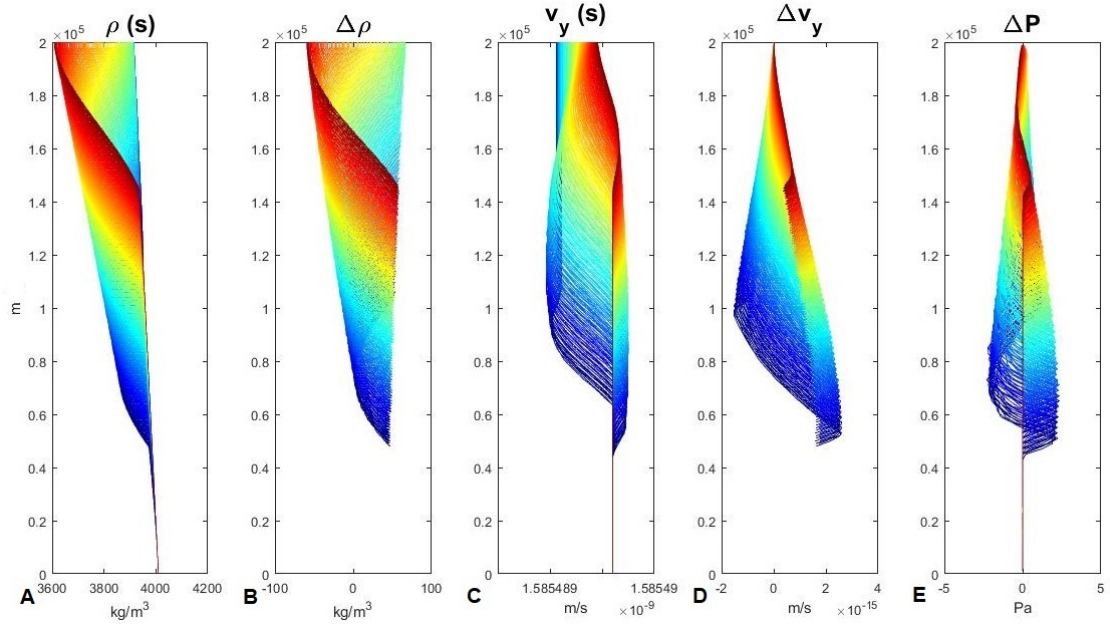


FIGURE 4.2: Incompressible non-turbulent evolution with depth of fluid variables, particularly, (A) Solid density ρ_s , (B) density difference $\Delta\rho = \rho_s - \rho_f$, (C) solid velocity \mathbf{v}_s , (D) velocity difference $\Delta\mathbf{v} = \mathbf{v}_s - \mathbf{v}_f$ and (E) pressure difference $\Delta P = P_s - P_f$.

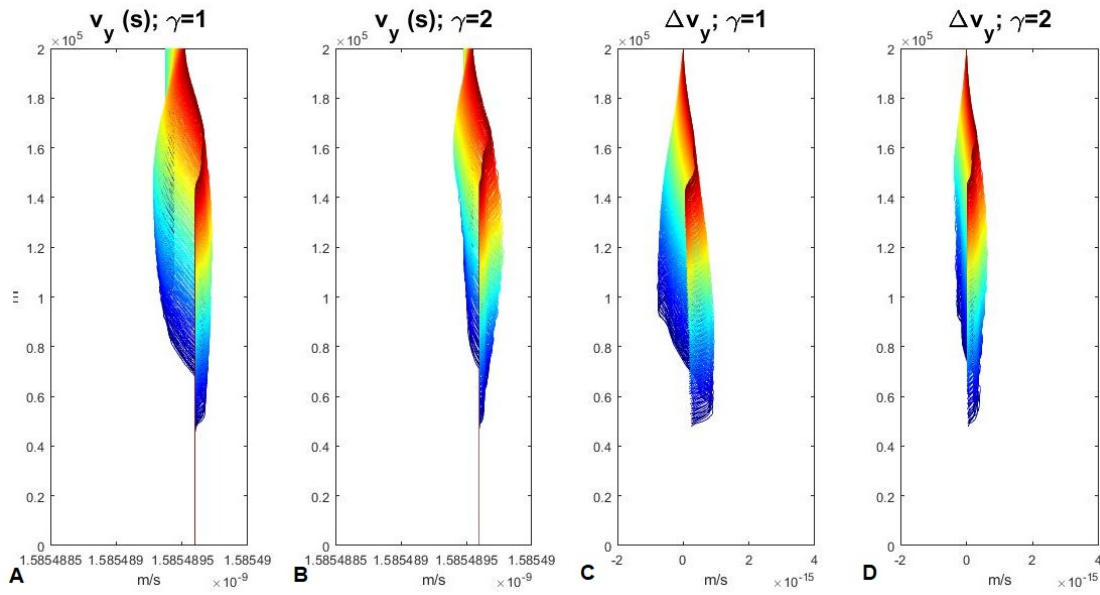


FIGURE 4.3: Incompressible turbulent evolution with depth of fluid variables, particularly, (A) solid velocity \mathbf{v}_s with $\gamma = 1$, (B) solid velocity \mathbf{v}_s with $\gamma = 2$, (C) velocity difference $\Delta \mathbf{v} = \mathbf{v}_s - \mathbf{v}_f$ for $\gamma = 1$ and (D) velocity difference $\Delta \mathbf{v} = \mathbf{v}_s - \mathbf{v}_f$ for $\gamma = 2$.

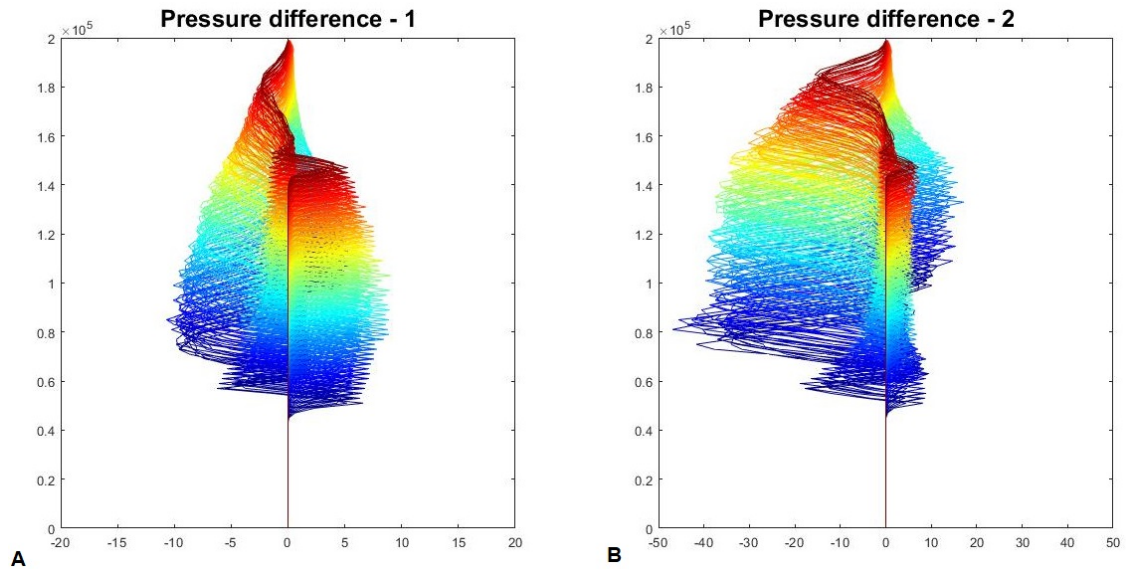


FIGURE 4.4: Incompressible turbulent evolution with depth of fluid variables, particularly, (A) pressure difference $\Delta P = P_s - P_f$ for $\gamma = 1$ and (B) pressure difference $\Delta P = P_s - P_f$ for $\gamma = 2$.

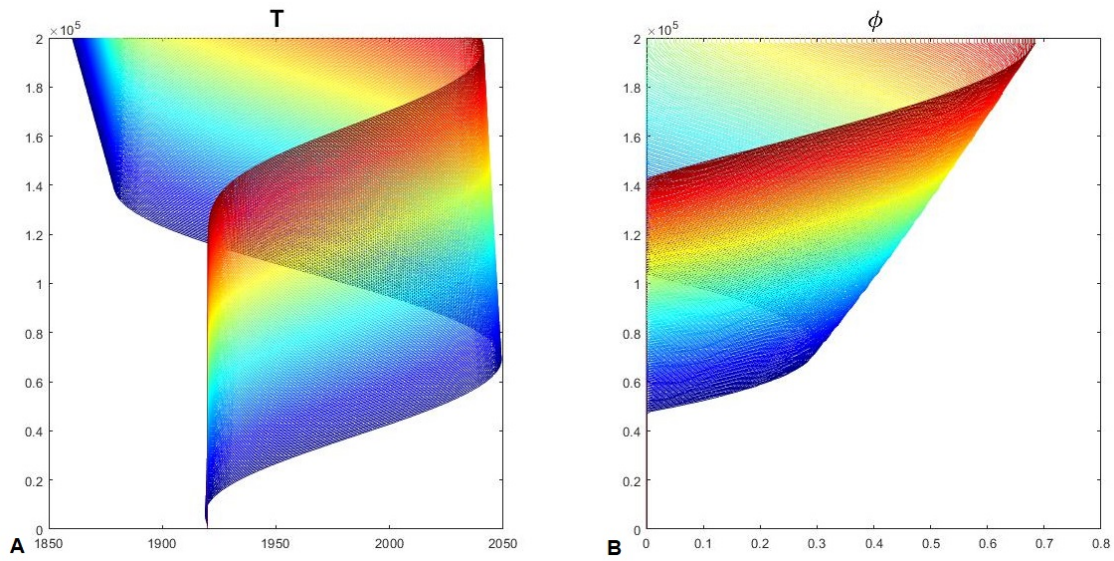


FIGURE 4.5: Compressible non-turbulent evolution with depth of fluid variables, particularly, (A) temperature T and (B) phase abundance ϕ .

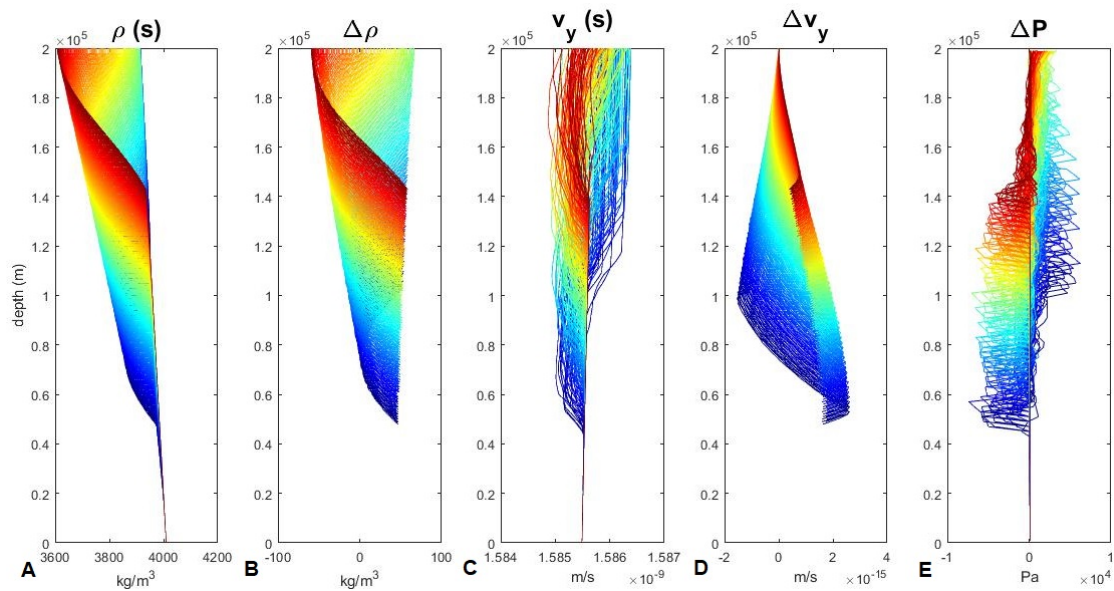


FIGURE 4.6: Compressible non-turbulent evolution with depth of fluid variables, particularly, (A) solid density ρ_s , (B) density difference $\Delta\rho = \rho_s - \rho_f$, (C) solid velocity \mathbf{v}_s , (D) velocity difference $\Delta\mathbf{v} = \mathbf{v}_s - \mathbf{v}_f$ and (E) pressure difference $\Delta P = P_s - P_f$ (particularly note the change in axes).

5

Conclusion & Discussion

In this thesis, a full set of compressible equations describing flow of averaged velocity, pressure and either temperature or entropy has been derived. The equations describe a system with an arbitrary number of phases and components, as well as dimensions. They were averaged using the ensemble averaging approach (Chapter 2), with the emerging turbulence terms treated in Section 3.3. The mathematical representation is general enough that it may be used as a shell for study of a variety of problems in geophysical fluid dynamics, with or without turbulence.

In Chapter 4, the equations were applied to some steady-state examples, particularly: (1) incompressible with no turbulence, (2) incompressible with turbulence and (3) compressible with no turbulence. Comparing (1) and (2), one can see that by including turbulence, the

velocity becomes dampened and as a consequence the pressure difference increases dramatically (see pressure jump conditions posed by Bercovici et al. [5], Sramek [9], Keller [48] and Oliveira et al. [11]). Comparing (1) and (3), one could see that while the melt content and temperature remain similar, densities and velocities experience some change, while the pressure difference undergoes a comparably huge change. Since the fluid is far more compressible than the solid, it makes sense that the fluid pressure takes the weight of the compressible system.

In both a turbulent and compressible system it was seen that the pressure difference is significantly larger than in the incompressible case. This implies that if the incompressible, non-turbulent scheme is used in an unsuitable application, results for field variable evolution may contain significant error. In particular, if the system is plastic, there may be some unanticipated volumetric fracturing [48].

In the future, numerical implementation could be expanded to solve non-steady state problems of higher dimension and with established turbulence models. The gap between incompressibility and compressibility should widen in the unsteady case, as a time-derivative forms part of the material derivative of density. As for the mathematical model, the turbulent aspects stand to improve significantly. Firstly, closing the system with the $T'' = 0$ assumption relaxed in the entropy equation (Section 3.1.4). Secondly, implementation of one or two-equation turbulence models into the multi-phase scheme. Thirdly, revision of the model such that the logic of Appendix A.1 is unnecessary, that is, never neglecting $\frac{\overline{\chi_k \rho' f'}}{\chi_k \hat{\rho} f}$ where f is a field variable; alternatively, providing a thorough analytical reasoning for the assumption may suffice. Clear improvements may also be made for the surface stress model: a visco-elastic plastic model is preferred over the viscous stress used here (see Section 3.2). Including elasticity using a Maxwell model (see Schubert [24]) and plasticity using an "effective viscosity approach" (e.g. Moresi [49], Kaus [50] and Keller [48]) is a logical next step. Oliveira et al. [11] provide implementation of visco-elastic plasticity into the incompressible multiphase ensemble averaged scheme.



Averaging Properties

A.1 Interchanging Phase- and Mass-Weightings

Consider the definition of an arbitrary mass-weighted variable:

$$\tilde{f} = \frac{\overline{\chi_k \rho f}}{\overline{\chi_k \hat{\rho}}} \quad (\text{A.1})$$

where an over-line indicates regular average; hat phase-weighted and tilde mass-weighted averages. Expanding ρ and f

$$\tilde{f} = \frac{\overline{\chi_k (\hat{\rho} + \rho') (\hat{f} + f')}}{\overline{\chi_k \hat{\rho}}} = \frac{\overline{\chi_k \hat{\rho} \hat{f}}}{\overline{\chi_k \hat{\rho}}} + \frac{\overline{\chi_k \rho' f'}}{\overline{\chi_k \hat{\rho}}} \quad (\text{A.2})$$

which follows because $\overline{\chi_k \hat{\rho} f'} = 0$ and $\overline{\chi_k \hat{f} \rho'} = 0$ by definition of Reynolds decomposition.

Dividing each side of Equation (A.2) by \hat{f}

$$\frac{\tilde{f}}{\hat{f}} = 1 + \frac{\overline{\chi_k \rho' f'}}{\overline{\chi_k \hat{\rho} \hat{f}}} \quad (\text{A.3})$$

thus, if the average of the product of fluctuations $\overline{\chi_k \rho' f'}$ is negligible with respect to the product of averaged variables $\chi_k \hat{\rho} \hat{f}$, then the phase-weighted temperature may be replaced by mass-weighted temperature $\tilde{f} \approx \hat{f}$.

A.2 Fluctuation Products

The averages of the fluctuations terms is zero; $\langle \chi_k \rho \theta'' \rangle = 0$ and $\langle \chi_k \theta'' \rangle = 0$.

This can be shown quite easily. The ensemble average of the fluctuation term is zero by definition, as can be seen by averaging either side of the following (and noting $\langle \langle \theta \rangle \rangle = \langle \theta \rangle$)

$$\theta = \langle \theta \rangle + \theta''. \quad (\text{A.4})$$

We want to show that the phase and mass weighted fluctuation terms are zero too. Starting from the definition of a mass-weighted average of the field variable (Equation 3.2)

$$\begin{aligned} \langle \chi_k \rho \rangle \langle \theta \rangle_\rho &= \langle \chi_k \rho \theta \rangle \\ &= \langle \chi_k \rho (\langle \theta \rangle_\rho + \theta'') \rangle \\ &= \langle \rho \langle \theta \rangle \rangle_\rho + \langle \chi_k \rho \theta'' \rangle \\ &= \langle \chi_k \rangle \langle \rho \rangle_\chi \langle \theta \rangle_\rho + \langle \chi_k \rho \theta'' \rangle \end{aligned} \quad (\text{A.5})$$

It is left to show the second term on the right-hand side is zero. By definition of the mass-weighted average of θ in Equation (3.2)

$$\langle \chi_k \rho \theta'' \rangle = \langle \chi_k \rho \rangle \langle \theta'' \rangle_\rho = \langle \chi_k \rangle \langle \rho \rangle_\chi \langle \theta'' \rangle_\rho = 0 \quad (\text{A.6})$$

Similarly, it can be shown using Equation (3.1)

$$\langle \chi_k \theta'' \rangle = 0 \quad (\text{A.7})$$

It is of interest to apply this property to a term of the form $(\langle \mathbf{v} \rangle_\rho + \mathbf{v}'')(\langle \mathbf{v} \rangle_\rho + \mathbf{v}'')$ as in Equation (3.17)

$$\langle (\langle \theta \rangle + \theta'')(\langle \theta \rangle + \theta'') \rangle = \langle \langle \theta \rangle \langle \theta \rangle + \langle \theta \rangle \theta'' + \theta'' \langle \theta \rangle + \theta'' \theta'' \rangle = \langle \theta \rangle \langle \theta \rangle + \theta'' \theta'' \quad (\text{A.8})$$

because $\langle \theta'' \langle \theta \rangle \rangle = \langle \theta'' \rangle \langle \theta \rangle = 0$ because $\langle \theta'' \rangle = 0$.

References

- [1] D. McKenzie. *The generation and compaction of partially molten rock*. Journal of Petrology **25**(3), 713 (1984).
- [2] N. M. Ribe. *The generation and composition of partial melts in the earth's mantle*. Earth and Planetary Science Letters **73**(2-4), 361 (1985).
- [3] F. M. Richter and D. McKenzie. *Dynamical models for melt segregation from a deformable matrix*. The Journal of Geology **92**(6), 729 (1984).
- [4] M. Spiegelman, R. Katz, and G. Simpson. *An introduction and tutorial to the mckenzie equations for magma migration*. Preprint, Columbia University, Dept. of Applied Physics and Applied Mathematics (2007).
- [5] D. Bercovici, Y. Ricard, and G. Schubert. *A two-phase model for compaction and damage: 1. general theory*. Journal of Geophysical Research: Solid Earth **106**(B5), 8887 (2001).
- [6] Y. Ricard, D. Bercovici, and G. Schubert. *A two-phase model for compaction and damage: 2. applications to compaction, deformation, and the role of interfacial surface tension*. Journal of Geophysical Research: Solid Earth **106**(B5), 8907 (2001).
- [7] D. Bercovici, Y. Ricard, and G. Schubert. *A two-phase model for compaction and damage: 3. applications to shear localization and plate boundary formation*. Journal of Geophysical Research: Solid Earth **106**(B5), 8925 (2001).

- [8] D. Bercovici and Y. Ricard. *Energetics of a two-phase model of lithospheric damage, shear localization and plate-boundary formation*. Geophysical Journal International **152**(3), 581 (2003).
- [9] O. Šrámek, Y. Ricard, and D. Bercovici. *Simultaneous melting and compaction in deformable two-phase media*. Geophysical Journal International **168**(3), 964 (2007).
- [10] S. R. De Groot and P. Mazur. *Non-equilibrium thermodynamics* (Courier Corporation, 2013).
- [11] B. Oliveira., J. C. Afonso, S. Zlotnik, and P. Diez. *Numerical modelling of multi-phase multi-component reactive transport in the earth's interior*. Geophysical Journal International (in press).
- [12] R. A. Lange and I. S. Carmichael. *Densities of na₂o-k₂o-cao-mgo-feo-fe₂o₃-al₂o₃-tio₂-sio₂ liquids: new measurements and derived partial molar properties*. Geochimica et Cosmochimica Acta **51**(11), 2931 (1987).
- [13] D. A. Drew and S. L. Passman. *Theory of multicomponent fluids*, vol. 135 (Springer Science & Business Media, 2006).
- [14] M. Kang, R. P. Fedkiw, and X.-D. Liu. *A boundary condition capturing method for multiphase incompressible flow*. Journal of Scientific Computing **15**(3), 323 (2000).
- [15] A. S. Monin and A. M. Yaglom. *Statistical fluid mechanics, volume II: Mechanics of turbulence*, vol. 2 (Courier Corporation, 2013).
- [16] M. Ishii and T. Hibiki. *Thermo-fluid dynamics of two-phase flow* (Springer Science & Business Media, 2010).
- [17] D. A. Drew. *Mathematical modeling of two-phase flow*. Annual review of fluid mechanics **15**(1), 261 (1983).
- [18] J.-W. Park, D. Drew, and R. Lahey Jr. *The analysis of void wave propagation in adiabatic monodispersed bubbly two-phase flows using an ensemble-averaged two-fluid model*. International Journal of Multiphase Flow **24**(7), 1205 (1999).

-
- [19] D. D. Joseph, T. S. Lundgren, R. Jackson, and D. Saville. *Ensemble averaged and mixture theory equations for incompressible fluidparticle suspensions*. International journal of multiphase flow **16**(1), 35 (1990).
- [20] B. V. Gnedenko. *The theory of probability and the elements of statistics*, vol. 132 (American Mathematical Soc., 2005).
- [21] J. L. Doob. *Measure theory*, vol. 143 (Springer Science & Business Media, 2012).
- [22] Y. Ricard. *Physics of mantle convection*. Mantle Dynamics, Treatise on Geophysics **7**, 31 (2009).
- [23] P. W. Atkins. *Physical chemistry. 1990*. There is no corresponding record for this reference (1978).
- [24] G. Schubert, D. L. Turcotte, and P. Olson. *Mantle convection in the Earth and planets* (Cambridge University Press, 2001).
- [25] P. Kundu and L. Cohen. *Fluid mechanics, 638 pp*. Academic, Calif (1990).
- [26] G. K. Batchelor. *An introduction to fluid dynamics* (Cambridge university press, 2000).
- [27] R. Aris. *Vectors, tensors and the basic equations of fluid mechanics* (Courier Corporation, 2012).
- [28] H. Tennekes and J. L. Lumley. *A first course in turbulence* (MIT press, 1972).
- [29] D. C. Wilcox *et al.* *Turbulence modeling for CFD*, vol. 2 (DCW industries La Canada, CA, 1998).
- [30] S. J. Kline, D. E. Coles, and E. Hirst. *Computation of turbulent boundary layers—1968 AFOSR-IFP-Stanford Conference: proceedings held at Stanford University, August 18-25, 1968*, vol. 1 (Thermosciences Division, Stanford University, 1969).
- [31] W. Lazeroms. *Turbulence modelling applied to the atmospheric boundary layer*. Ph.D. thesis, KTH Royal Institute of Technology (2015).

-
- [32] S. B. Pope. *Turbulent flows* (2001).
- [33] S. W. Churchill. *A reinterpretation of the turbulent prandtl number*. Industrial & engineering chemistry research **41**(25), 6393 (2002).
- [34] F. M. White and I. Corfield. *Viscous fluid flow*, vol. 3 (McGraw-Hill Higher Education Boston, 2006).
- [35] S. Sarkar, G. Erlebacher, M. Hussaini, and H. Kreiss. *The analysis and modelling of dilatational terms in compressible turbulence*. Journal of Fluid Mechanics **227**, 473 (1991).
- [36] S. Sarkar and B. Lakshmanan. *Application of a reynolds stress turbulence model to the compressible shear layer*. AIAA journal **29**(5), 743 (1991).
- [37] W. Jones and B. Launder. *The prediction of laminarization with a two-equation model of turbulence*. International journal of heat and mass transfer **15**(2), 301 (1972).
- [38] C. Simonin and P. Violette. *Predictions of an oxygen droplet pulverization in a compressible subsonic coflowing hydrogen flow*. Numerical Methods for Multiphase Flows, FED91 pp. 65–82 (1990).
- [39] A. Troshko and Y. Hassan. *A two-equation turbulence model of turbulent bubbly flows*. International Journal of Multiphase Flow **27**(11), 1965 (2001).
- [40] A. Smith and T. Cebeci. *Numerical solution of the turbulent-boundary-layer equations*. Tech. rep., DOUGLAS AIRCRAFT CO LONG BEACH CA AIRCRAFT DIV (1967).
- [41] B. S. Baldwin and H. Lomax. *Thin layer approximation and algebraic model for separated turbulent flows*, vol. 257 (American Institute of Aeronautics and Astronautics, 1978).
- [42] H. Stock and W. Haase. *Determination of length scales in algebraic turbulence models for navier- stokes methods*. AIAA journal **27**(1), 5 (1989).
- [43] K.-J. Bathe. *Computational fluid and solid mechanics* (Springer, 2001).

-
- [44] P. R. Spalart, S. R. Allmaras, *et al.* *A one equation turbulence model for aerodynamic flows*. RECHERCHE AEROSPATIALE-FRENCH EDITION- pp. 5–5 (1994).
- [45] R. B. Bird. *Transport phenomena*. Applied Mechanics Reviews **55**(1), R1 (2002).
- [46] P. Vinet, J. H. Rose, J. Ferrante, and J. R. Smith. *Universal features of the equation of state of solids*. Journal of Physics: Condensed Matter **1**(11), 1941 (1989).
- [47] R. G. Berman. *Internally-consistent thermodynamic data for minerals in the system na₂o-k₂o-ca₂o-mg₂o-*feo*-*fe*₂*o*₃-*al*₂*o*₃-*sio*₂-*tio*₂-*h*₂*o*-*co*₂*. Journal of petrology **29**(2), 445 (1988).
- [48] T. Keller, D. A. May, and B. J. Kaus. *Numerical modelling of magma dynamics coupled to tectonic deformation of lithosphere and crust*. Geophysical Journal International **195**(3), 1406 (2013).
- [49] L. Moresi, F. Dufour, and H.-B. Mühlhaus. *A lagrangian integration point finite element method for large deformation modeling of viscoelastic geomaterials*. Journal of Computational Physics **184**(2), 476 (2003).
- [50] B. J. Kaus. *Factors that control the angle of shear bands in geodynamic numerical models of brittle deformation*. Tectonophysics **484**(1), 36 (2010).